Kansas Geological Survey

Approximate Analysis of Aquifer Mineralization Due to Horizontal Penetration of Salinity

By

Hillel Rubin* and Robert W. Buddemeier
Kansas Geological Survey, The University of Kansas
Lawrence, KS 66047

Kansas Geological Survey Open File Report 98-33
September 16, 1998

GEOHYDROLOGY

The University of Kansas, Lawrence, KS 66047 Tel.(785) 864-3965

Approximate Analysis of Aquifer Mineralization due to Horizontal Penetration of Salinity

Hillel Rubin[1] and Robert W. Buddemeier
Kansas Geological Survey, The University of Kansas
Lawrence, Kansas 66047,

Abstract

This report describes techniques for analyzing the mineralization of groundwater resources due to horizontal penetration of saltwater into a freshwater aquifer. The methods were developed within the framework of a comprehensive research program concerning groundwater mineralization in south central Kansas. Previous studies addressed cases, in which a comparatively thin mineralized region represented by boundary layers (BLs) developed within the freshwater aquifer close to sources of salinity. However, at some distance downstream from the salinity source, the top of the mineralized region reaches the top of the aquifer. This is the location of the "attachment point", which comprises the entrance cross section of the domain evaluated by the present study. It is shown that downstream from the entrance cross section, a set of two BLs develop in the aquifer, termed inner and outer BLs. It is assumed that the evaluated domain, in which the salinity distribution gradually becomes uniform, can be divided into two sections, designated: (a) the restructuring section, and (b) the establishment section. In the restructuring section, the vertical salinity gradient leads to expansion of the inner BL at the expense of the outer BL, and there is almost no transfer of salinity between the two layers. In the establishment section, each of the BLs occupies half of the aquifer thickness, and the vertical salinity gradient leads to transfer of salinity from the inner to the outer BL. By use of BL approximations, changes of salinity distribution in the aquifer are calculated and evaluated. The establishment section ends at the uniformity point, downstream from which aquifer salinity is vertically uniform. The length of the restructuring section, as well as that of the establishment section, is approximately proportional to the aquifer thickness squared, and is inversely proportional to the transverse dispersivity.

The study provides a convenient set of definitions and terminology that are helpful in visualizing the gradual development of uniform salinity distribution in an aquifer subject to mineralization. The method developed in this study can be applied to a variety of problems associated with groundwater quality, such as initial evaluation of field data, design of field data collection, the identification of appropriate boundary conditions for numerical models, selection of appropriate numerical modeling approaches, interpretation and evaluation of field monitoring results, etc.

---

[1]On leave from Department of Civil Engineering, Technion - Israel Institute of Technology, Haifa 32000, Israel

Introduction

The aquifer within the Equus Beds Groundwater Management District in south central Kansas provides most of the fresh and usable water in that region. During the last three decades groundwater withdrawals have increased, leading to concerns about salinity intrusion into the aquifer. Major sources of salinity intrusion are the Arkansas River and saltwater occurring up-gradient in the neighboring Great Bend Prairie aquifer, as well as brines originating from oil field activities *(USBR, 1993; Whittemore and Sophocleous, 1995).* Various studies *(e.g., Buddemeier et al., 1993, 1994; Garneau, 1995; Rubin and Buddemeier, 1998a, b, c, d)* have addressed mineralization processes typical of the Great Bend Prairie aquifer. This aquifer is subject, in various locations, to seepage of saltwater originating from deep Permian formations saturated with saltwater. Direct contact between fresh and saltwater strata of the aquifer may also lead to transverse dispersion of salinity from the saltwater region into the freshwater zone.

In several previous studies *(Rubin and Buddemeier, 1996, 1998a, b, c, d)* the authors have developed the top specified boundary layer (TSBL) method and applied it to predict various types of scenarios possible in aquifer mineralization processes, with emphasis on south-central Kansas. In all these studies, it was assumed that the thickness of the aquifer is larger than the thickness of the mineralized zone that develops due to the penetration of salinity into the freshwater aquifer. According to the top specified boundary layer (TSBL) method, the region of interest (ROI), in which the salinity exceeds acceptable values, occupies a portion of the mineralized zone. In cases of aquifer thickness larger than the mineralized zone, the TSBL can be used to provide adequate information concerning the rate of growth of the ROI, its horizontal penetration into regions which were originally fresh, and variation of salinity distribution in the mineralized aquifer. However, during horizontal movement, the mineralized zone expands and reaches the top of the aquifer at a location called the "attachment point". Downstream from this point, the salinity distribution in the aquifer gradually becomes uniform. The objective of the present study is to provide simplified tools by which an appropriate description of this process is provided. It is also anticipated that simplified expressions can be obtained to estimate the characteristic length scale over which the

uniformity of salinity distribution in the aquifer is obtained. The results will be useful in initial evaluation and interpretation of field data, and in selecting appropriate numerical models aimed at more sophisticated simulation of transport phenomena in the aquifer.

Conceptual modeling

The basic conceptual model applied in this study is shown in Fig. 1. We assume that the aquifer can be represented as a layer of finite thickness of a porous medium saturated with freshwater. Salinity intrusion occurs at a discontinuity in the impermeable layer representing the bottom of the aquifer. The length of the discontinuity is X_e^*. The salinity may enter the freshwater region either due to direct contact between fresh and saltwater *(Rubin and Buddemeier, 1998a, c)* or due to seepage of saltwater originating from difference of potentiometric head between the salt and freshwater zones *(Rubin and Buddemeier, 1998b, d)*. The salinity intrusion causes the build-up of the mineralized zone and its expansion along the aquifer of thickness B^* until its top ordinate reaches the top of the aquifer at the attachment point. The distance between the upstream end of the impermeable layer discontinuity and the attachment point is X_{ent}^*. Previous studies of the authors *(Rubin and Buddemeier, 1998a, b, c, d)* have indicated that various types of BL approaches can simulate the mineralized zone. In the previous studies, the top ordinate of the mineralized zone represents the vertical distance from the bottom of the aquifer to the location in which the salt concentration (salinity) is about one thousand times smaller than that of the saltwater region. The region of interest (ROI) can be considered to be the transition zone between fresh and saltwater. It occupies the portion of the mineralized zone, in which the salinity exceeds acceptable values. For the purpose of this study, we consider that the top of the ROI represents an isohaline of one percent of the salinity of the saltwater.

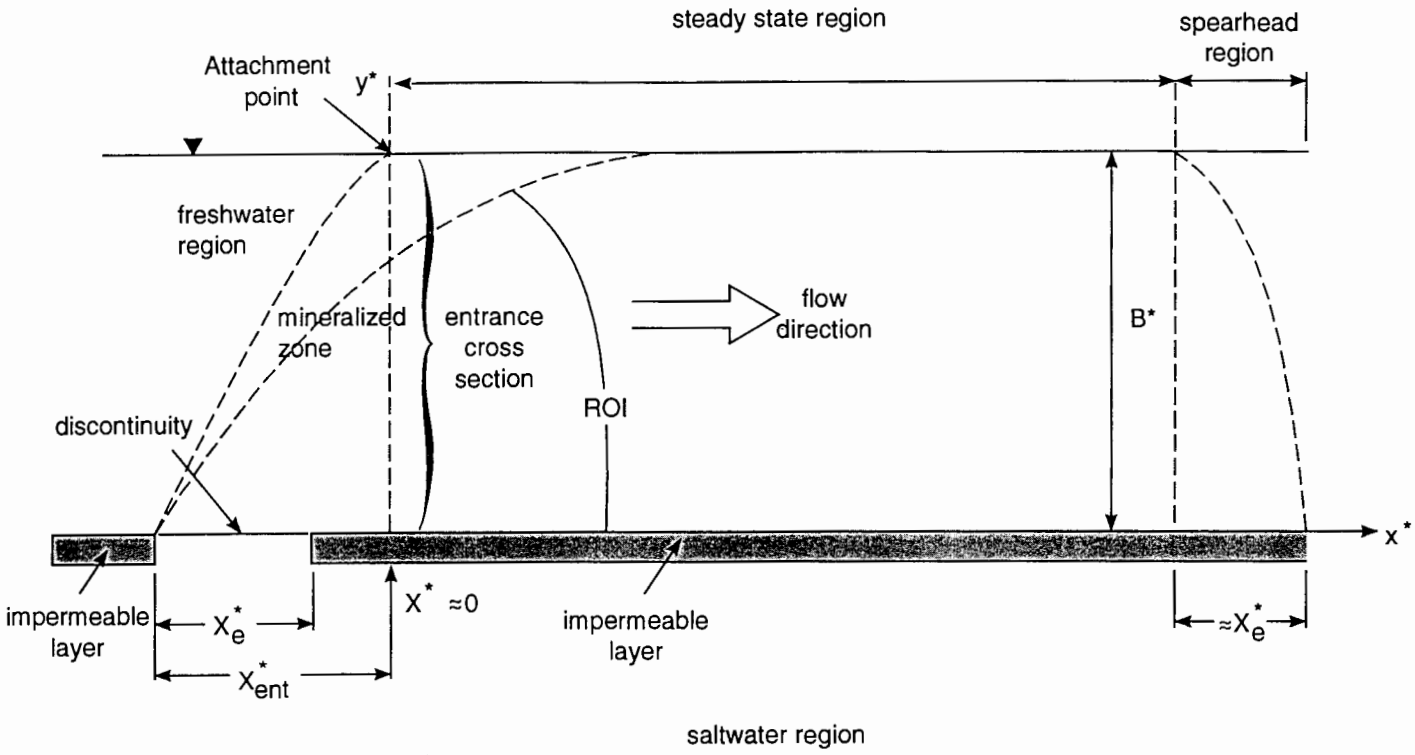

Figure 1 The conceptual model of aquifer mineralization, showing the terms and qualitative spatial relationships of the features. ROI = Region of Interest.

Previous studies *(Rubin and Buddemeier, 1998c, d)* showed that downstream of the impermeable layer discontinuity in an infinite (very thick) aquifer the horizontal penetration of salinity consists of two regions: (a) the spearhead region, and (b) the steady state region. The length of the spearhead region is identical to the length of the impermeable layer discontinuity, i.e. X_e^*. This region is subject to vertical expansion while it is advected horizontally in the aquifer. In the steady state region, salinity distribution is subject to steady state conditions. It is sometimes possible to use available analytical solutions of the heat transfer equation *(Carslaw and Jaeger, 1959; Hill and Dewynne, 1987)* to describe the salinity distribution in the steady state region, because of analogies between problems of heat transfer and the transfer of salinity in the aquifer. The analogy is between salinity distribution in the infinite aquifer and temperature distribution in an insulated semi-infinite slab with a given initial temperature distribution. The longitudinal coordinate of the aquifer replaces the time coordinate of the heat transfer problem, and the vertical coordinate replaces the longitudinal coordinate of the heat transfer problem. The initial temperature distribution is analogous to the salinity distribution in a defined entrance cross section of the aquifer domain. However, use of the analytical solution analogy becomes complicated when we refer to typical entrance salinity profiles.

In the case of a finite aquifer, again we may use the analytical solution analogy between salinity distribution in the steady state region and temperature distribution in an insulated slab whose initial temperature distribution is given. However, again reference to real typical entrance salinity distributions makes the analytical calculations complicated. Another approach to the development of analytical solutions is to consider the discontinuity of the impermeable layer as a point source. Then top and bottom of the aquifer can be simulated by using the image method (e.g. Fischer et al., 1979). However, such an approach can be inadequate in practical cases of even minor non-uniformity of the domain, and cannot refer to every possible salinity profile at the entrance of the domain. Therefore, for the purpose of the present study, we tested the possible use of the BL approach with numerical simulations.

As long as salinity gradients in the vertical direction are much larger than the horizontal ones, we may ignore effects of longitudinal dispersion in the domain. Such neglect is probably valid in the steady state region. However, in the spearhead region, effects of longitudinal dispersion may be significant. This region may also be subject to shrinkage at its upstream end due to the finite thickness of the aquifer. Because these effects are limited to a comparatively small region, the present study addresses issues associated only with the steady state region while considering that mineralization of the aquifer propagates with the salinity advection velocity. Therefore, our calculations concern changes of salinity distribution in the domain between the entrance cross section and the spearhead region, i.e. the steady state region.

Basic formulation

Flow conditions and salinity transport in the complete domain of Fig. 1 are governed by the following set of differential equations

$$\vec{q} = -\frac{k}{\mu}(\nabla p - \rho \vec{g}) \tag{1}$$

$$\frac{\partial C^*}{\partial t^*} + \vec{V} \cdot \nabla C^* = \nabla \cdot (\tilde{D} \cdot \nabla C^*) \tag{2}$$

where $\vec{q}$ is the specific discharge vector, k is the permeability, μ is the fluid viscosity, p is the pressure, ρ is the fluid density, g is the gravitational acceleration, C^* is the salt concentration (salinity), V is the interstitial flow velocity, D is the dispersion tensor, and t^* is time.

Equations. (1) and (2) represent a set of differential equations, which can be solved by various types of numerical procedures (e.g. *Reeves et al., 1986).* However, the simultaneous solution of eqs. (1) and (2) is quite complicated; the nonlinearity stemming from the dependence of ρ on C^* introduces simulation difficulties, and there are problems of stability of the numerical solution, numerical dispersion, etc. Therefore, simplification

of the calculation of salinity transport in the domain of Fig. 1 is very desirable. We consider that flow in the aquifer is mainly in the horizontal direction and the aquifer thickness is constant. Such an assumption is not required by the BL approach, but it simplifies the calculations. This assumption is completely acceptable if the top of the aquifer can be treated as an impermeable layer. For the free-surface aquifer we can apply the Dupuit approximation and consider some variations in the aquifer thickness and the flow velocity. As flow is basically horizontal, we may neglect effects of density stratification on the initial uniform velocity distribution in the domain. We adopt a coordinate system, as shown in Fig. 1, whose origin is located at the entrance cross section. The horizontal (longitudinal) x^* axis is extended along the impermeable bottom of the aquifer. The vertical, y^* axis represents the entrance cross section.

Due to the negligible effect of salinity on the flow velocity we use the solution of eq. (2). When the flow velocity field is already given, e.g. by considering the Dupuit approximation, we obtain

$$\frac{\partial C^*}{\partial t^*} + V\frac{\partial C^*}{\partial x^*} = D_x\frac{\partial^2 C^*}{\partial x^{*2}} + D_y\frac{\partial^2 C^*}{\partial y^{*2}} \tag{3}$$

where x^* and y^* are the longitudinal and vertical coordinates, respectively, and D_x and D_y are the longitudinal and transverse dispersion coefficients, respectively.

However, the effect of longitudinal dispersion can be neglected as long as salinity gradients in the vertical direction are much larger than gradients in the horizontal direction. Therefore, the first right-hand term of eq. (3) can be neglected. Also for quite long distances we may assume constant flow velocity. Therefore, it is appropriate to apply dimensionless coordinates and variables given by

$$x = \frac{x^*}{l_0}; \quad y = \frac{y^*}{l_0}; \quad t = \frac{t^* V}{l_0}; \quad C = \frac{C^* - C_f^*}{C_s^* - C_f^*} \tag{4}$$

where l_0 is an adopted unit length, and C_f^* and C_s^* are values of the salinity in the fresh and saltwater, respectively.

Introducing the dimensionless variables of eq. (4) into eq. (3) we obtain

$$\frac{\partial C}{\partial t}+\frac{\partial C}{\partial x}=a\frac{\partial^2 C}{\partial y^2} \tag{5}$$

where a is the dimensionless transverse dispersivity. This variable is defined by

$$a=\frac{D_y}{l_0 V} \tag{6}$$

It is assumed that dispersion coefficients are proportional to the flow velocity. Therefore, a is a constant coefficient.

Other important geometrical parameters subject to nondimensionalization are given by

$$X_e=\frac{X_e^*}{l_0};\quad X_{ent}=\frac{X_{ent}^*}{l_0};\quad B=\frac{B^*}{l_0} \tag{7}$$

Figure 2 shows the terms and symbols used in this development, and the initial and boundary conditions of the domain subject to evaluation. These conditions may be expressed in terms of dimensionless variables, given by:

$$C=C(x,y,t),\quad x,y,t\geq 0 \tag{8}$$

$$\frac{\partial C}{\partial y}=0\quad at\quad y=0 \tag{9}$$

$$\frac{\partial C}{\partial y} = 0 \quad at \quad y = B \tag{10}$$

$$C(0, y, t) = C(y, t) \tag{11}$$

At $t = X_{ent}$ the salinity profile at the entrance cross section is established and obtains its steady state value. Then the boundary condition given by eq. (11) is changed to

$$C(0, y, t) = C(y) \tag{12}$$

Our major interest is in identifying the uniformity point, located at a distance X_p, downstream from the entrance cross section, at which the salinity distribution in the aquifer cross section becomes uniform. Therefore, we refer to steady state conditions by neglecting the spearhead region and considering that the entrance salinity profile, at the attachment point, is given by eq. (12).

Under steady state conditions eq. (5) collapses to

$$\frac{\partial C}{\partial x} = a\frac{\partial^2 C}{\partial y^2} \tag{13}$$

It should be noted that eq. (13) is applicable even when the flow velocity varies along the aquifer, e.g., in cases of a free surface aquifer, confined aquifer subject to contraction or expansion, variability of the aquifer porosity, etc. However, in such cases, changes of the aquifer parameters should be considered.

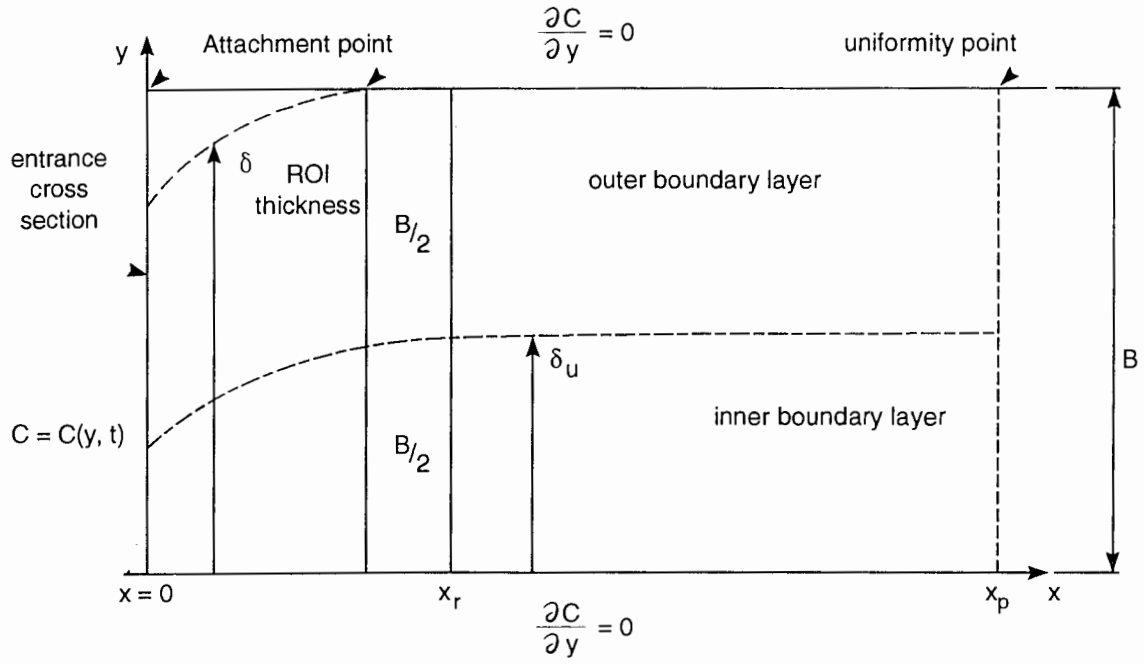

Figure 2 Schematic description of the evaluated domain in terms of the Top Specified Boundary Layer approach

Equation (13) is subject to the set of boundary conditions given by eqs. (9), (10) and (12). Such a system is completely analogous to the problem of heat transfer in a finite insulated slab with a given initial temperature distribution *(Carslaw and Jaeger, 1959; Hill and Dewynne, 1987).* Another analytical solution approach would be to consider the source of salinity as a line or point source and later use the image method (*e.g. Fischer et al., 1979)* to simulate the presence of the bottom and top of the aquifer. However, this method is limited in terms of its capability to deal with all of the types of salinity profiles, which may occur at the domain entrance. We intend to consider various realistic entrance salinity profiles characterizing possible scenarios of saltwater intrusion in Kansas, which may result in quite complicated calculations in the analytical formulations. Therefore, we apply a numerical simulation approach in two stages: a) a preliminary stage, aimed at the verification of the feasibility of using the BL approach, and b) an evaluation and calibration of the BL modeling approach. The following section describes the first stage of the numerical simulations.

Preliminary numerical experiments

We applied a Crank-Nicolson finite difference numerical scheme to the solution of eq. (13), subject to the boundary conditions of eqs. (9) and (10) and entrance salinity profiles characterizing several realistic cases of aquifer mineralization. In Fig. 3, two examples of such realistic entrance salinity profiles are provided. Fig. 3(a) shows a typical salinity profile originating from direct contact between fresh and saltwater at the impermeable layer discontinuity *(Rubin and Buddemeier, 1998c).* Fig. 3(b) shows a typical salinity profile originating from seepage of saltwater through the impermeable layer discontinuity *(Rubin and Buddemeier, 1998d).* In both cases we refer to a value of salinity at the top of the aquifer, C_t, which is equal to 0.1% of the salinity at the bottom of the aquifer, C_b.

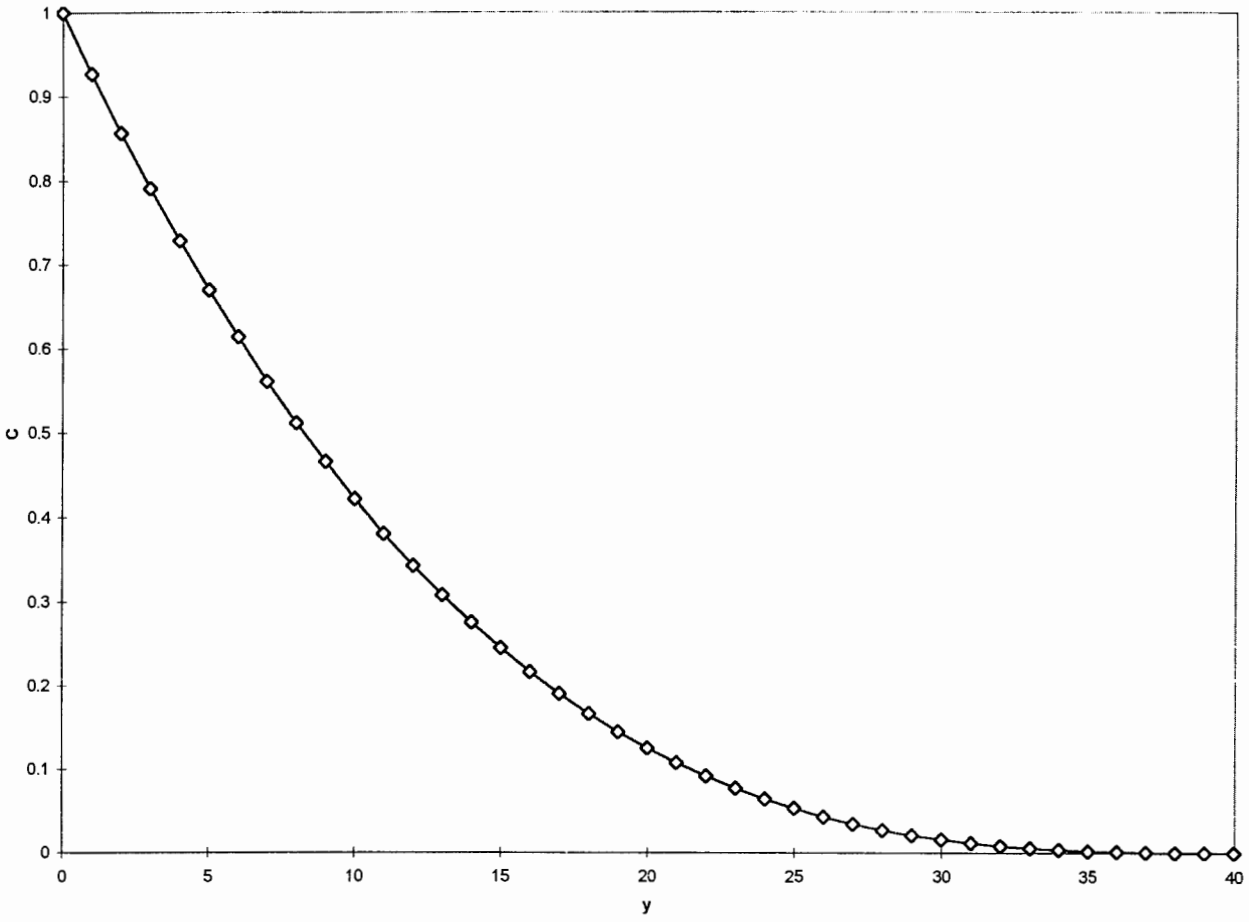

Figure 3a Types of entrance salinity profiles for two different types of saliniity sources and aquifers.

(a) Direct contact between fresh and saltwater *(B=40)*

($a=0.1$; X_e, X_{ent} = 1330) or ($a=0.5$; X_e, X_{ent} = 267)

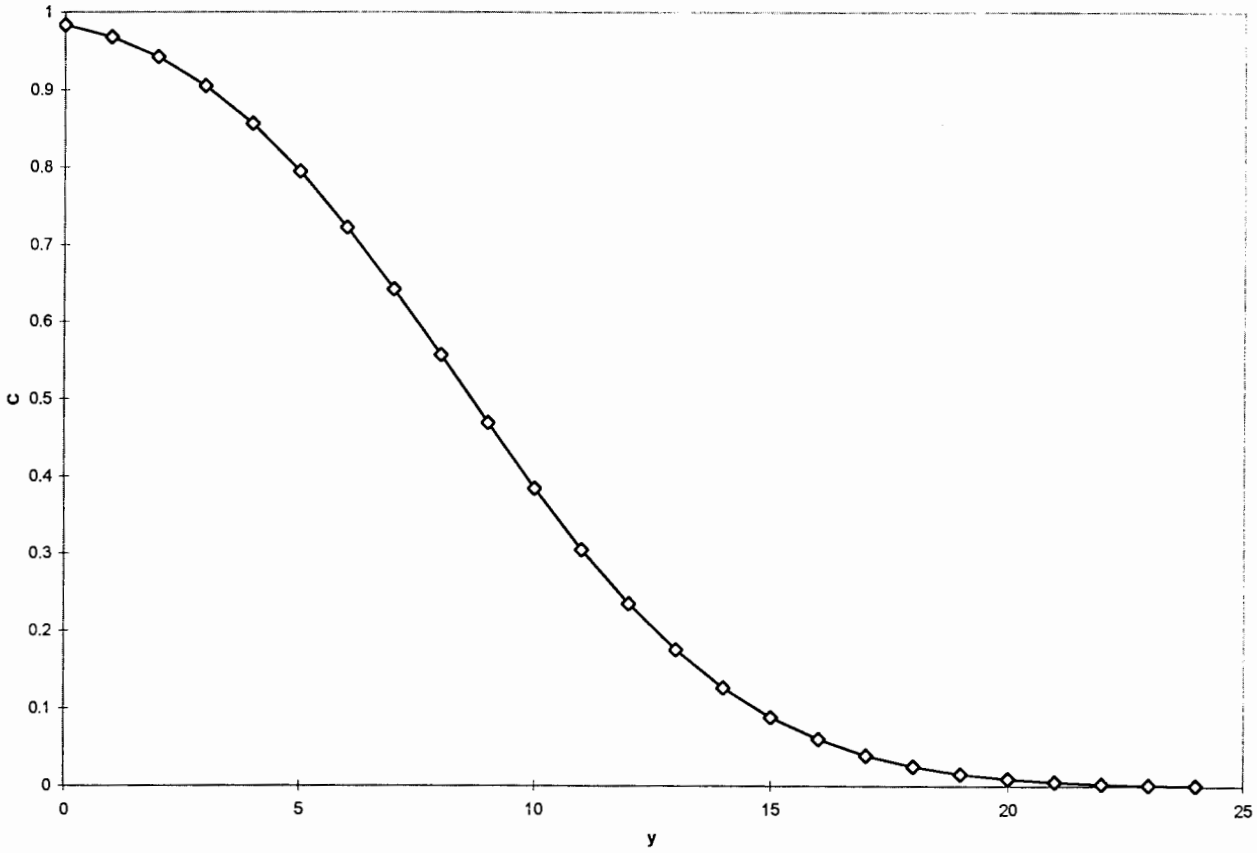

Figure 3b Types of entrance salinity profiles for two different types of saliniity sources and aquifers.

(b) Seepage of saltwater into the freshwater zone

($a=0.1$; $q_R=0.1$; X_e, $X_{ent}=100$; $B=24$)

We assume that the domain incorporates two BLs downstream of the entrance cross section at the attachment point. Figure 2 shows the two BLs developed in the domain: (a) the inner BL extending between the bottom of the aquifer and $y = \delta_u$, and (b) the outer BL extending between $y = \delta_u$ and $y = B$. The following paragraphs incorporate sample results of the numerical experiments by which we validated this assumption.

Application of a BL approach requires the ability to identify salinity profiles, (i.e. scaled salinity values versus scaled coordinates) which can represent the salinity distribution in extensive portions of the evaluated domain.

We assumed that normalized salinity values could be represented by the following expression

$$c = \frac{C - C_t}{C_b - C_t} \tag{14}$$

We assumed that the top of the inner BL, $y = \delta_u$, and the top of the region of interest (ROI), $y = \delta$, could be defined respectively by

$$y = \delta_u \quad where \quad c = 0.5 \tag{15}$$

$$y = \delta \quad where \quad C = 0.01 \tag{16}$$

By solving eq. (13) subject to the boundary conditions given by eq. (9), (10) and (12), we have obtained the salinity distribution in the evaluated domain. Then, applying eqs. (14) - (16) produced normalized salinity values and values of δ_u and δ. The results derived from this information are presented in Fig. 4. These results incorporate variation of δ_u and δ along the aquifer until uniformity of the salinity distribution in the vertical cross section is obtained at the point of uniformity, located at a distance X_p downstream from the attachment point at the entrance cross section. The achievement of a uniform salinity profile is defined by

$$C_b - C_t \leq 0.01 \tag{17}$$

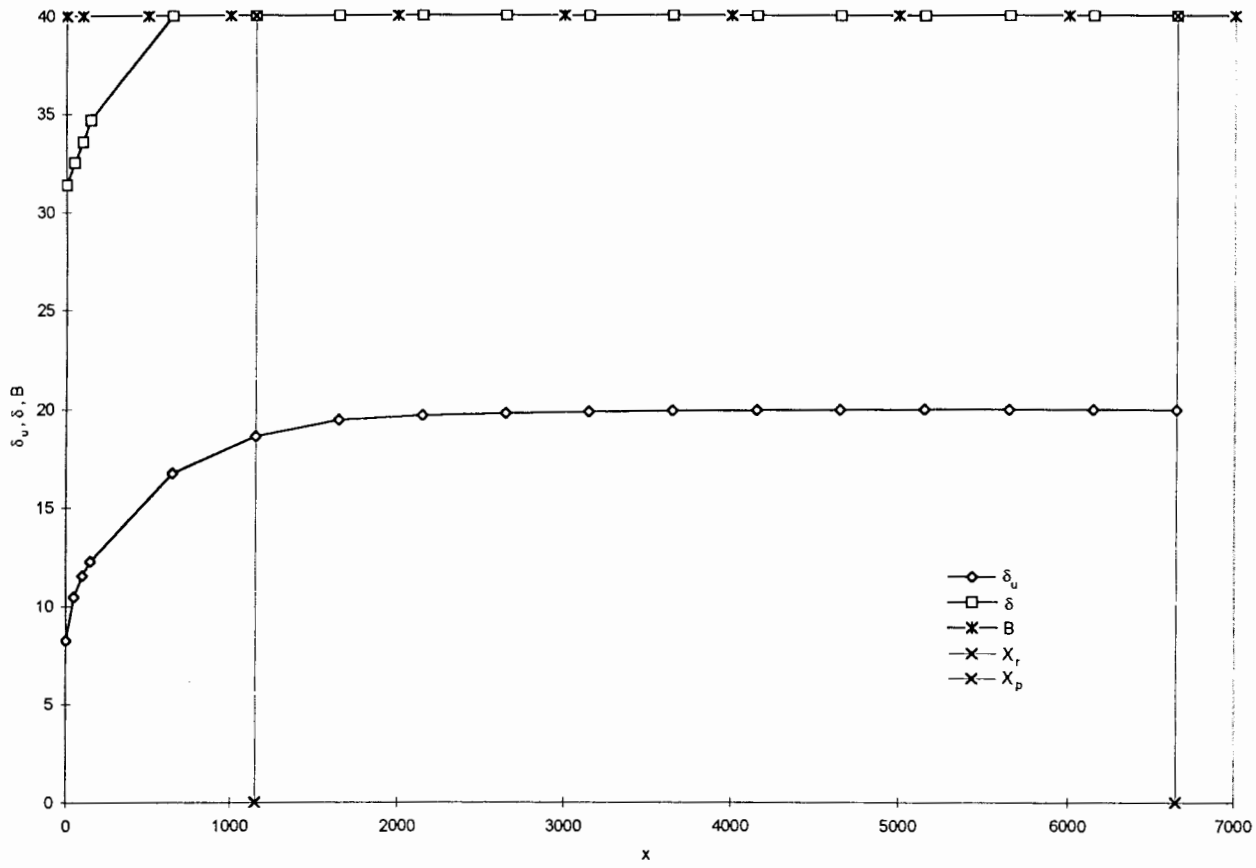

Figure 4a Variation of the boundary layer thickness along the aquifer - presentation of numerical results

(a) Direct contact between fresh and saltwater *(a=0.1; B=40)*

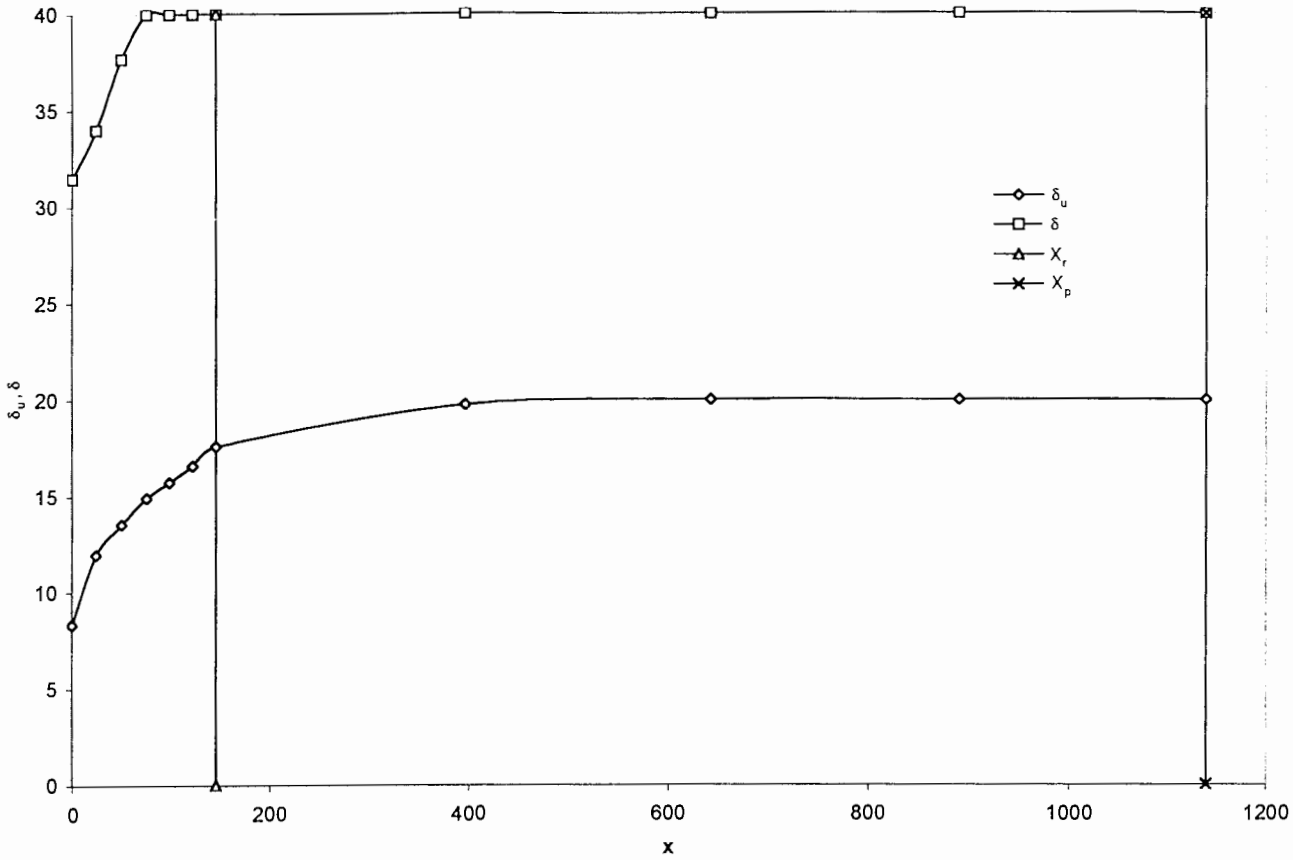

Figure 4b Variation of the boundary layer thickness along the aquifer - presentation of numerical results

(b) Direct contact between fresh and saltwater *(a=0.5; B=40)*

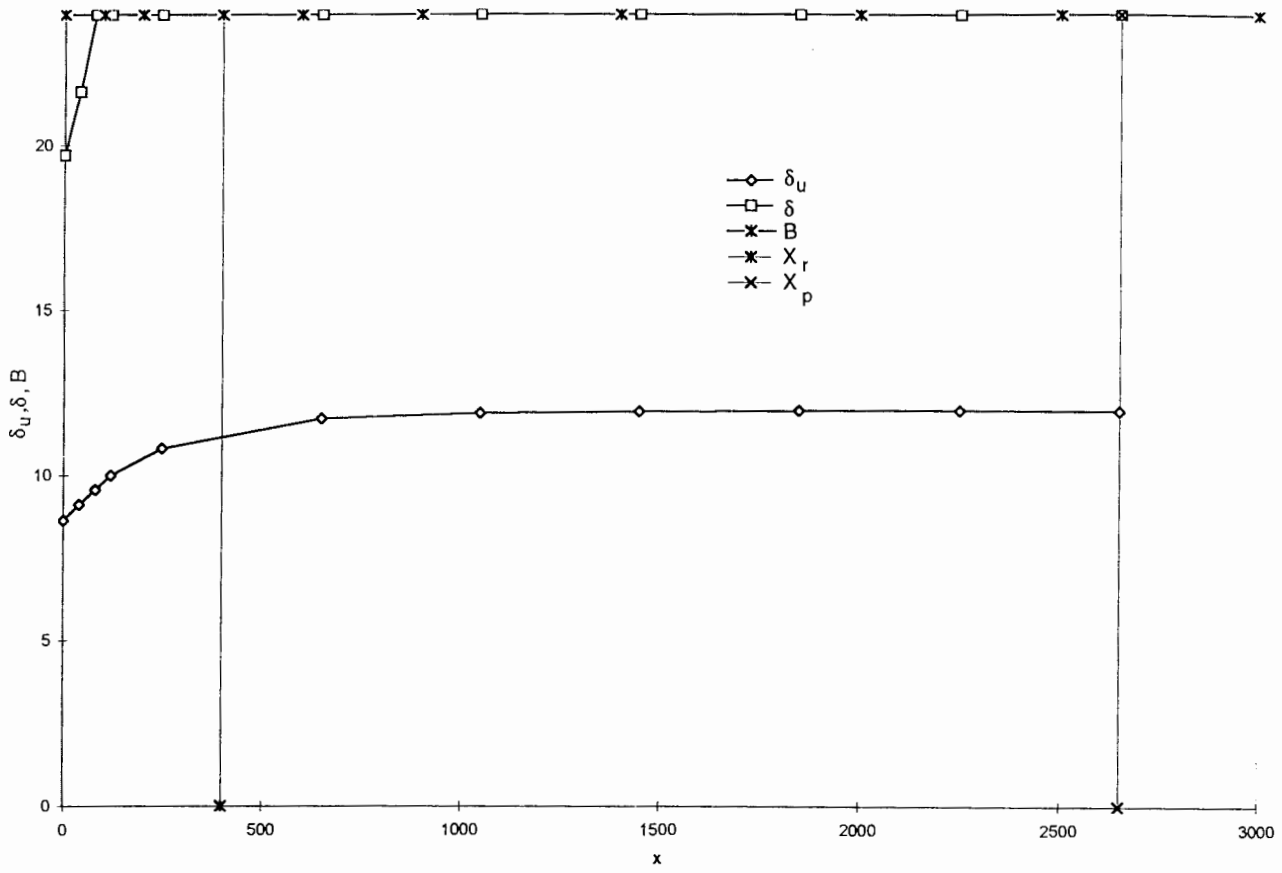

Figure 4c Variation of the boundary layer thickness along the aquifer - presentation of numerical results

(c) Seepage of saltwater into the freshwater zone

($a=0.1$; $q_R=0.1$; X_e, $X_{ent}=100$; $B=24$)

The results presented in Fig. 4 show that in a short distance downstream of the entrance cross section the ROI extends between the bottom and top of the aquifer. The value of δ_u gradually reached the value

$$\delta_u = B/2 \tag{18}$$

These results indicate that at a comparatively short distance X_r downstream of the entrance cross section, the thickness of the inner BL was about 90 percent of the value specified by eq. (18). Values of X_p and X_r were approximately related by

$$X_r = 0.15\, X_p \tag{19}$$

The adopted value of X_r is not uniquely given, and it can be associated with a reasonable value of δ_u larger than 90% of the value specified by eq. (18).

In Fig. 4, vertical lines show the approximate values of X_p and X_r.

Downstream from $x = X_r$ the inner BL thickness varied only slightly over a large distance.

Figure 5 shows how the value of C_b decreased, and the value of C_t increased along the aquifer, until both values became identical to the average salinity in the vertical cross section.

The validity of our basic assumption of the existence of inner and outer BLs, was evaluated by comparing the similarity of various salinity profiles in the domain to be evaluated. The following paragraphs describe this process.

We defined vertical coordinates ξ and η for the inner and outer BLs, respectively, as

$$\xi = \frac{\delta_u - y}{\delta_u} \quad at \quad 0 \le y \le \delta_u \tag{20}$$

$$\eta = \frac{y - \delta_u}{B - \delta_u} \quad at \quad \delta_u \le y \le B \tag{21}$$

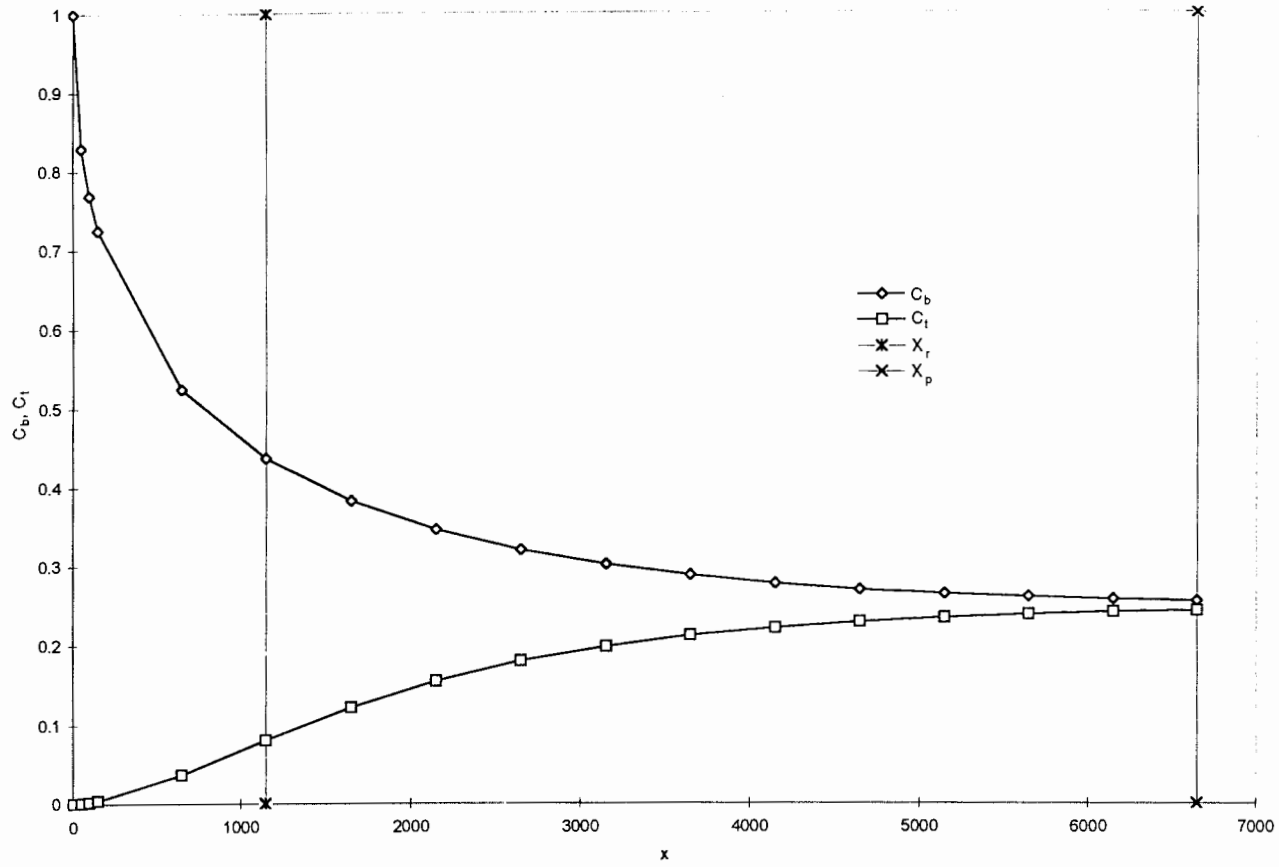

Figure 5a Variation of bottom and top salinity along the aquifer - presentation of numerical results

(a) Direct contact between fresh and saltwater *(a=0.1; B=40)*

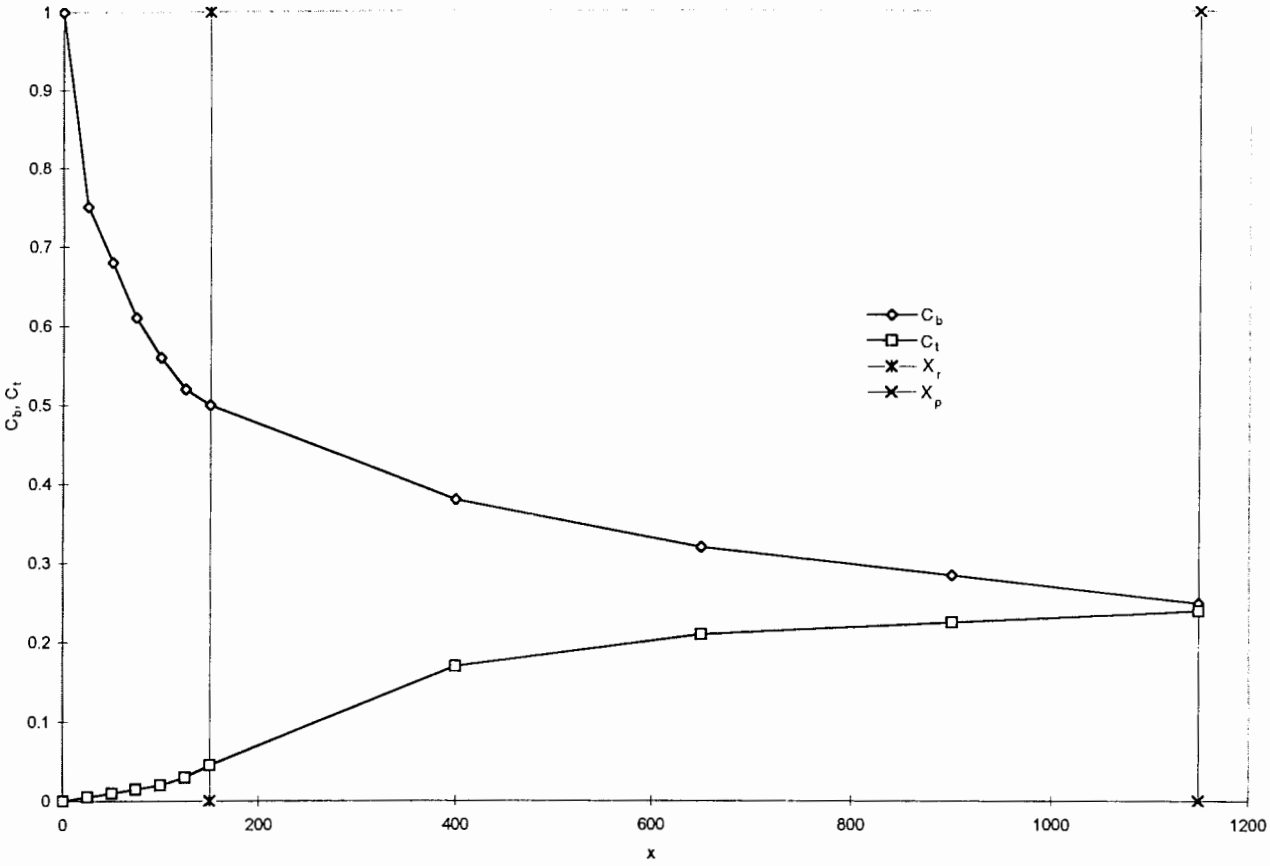

Figure 5b Variation of bottom and top salinity along the aquifer - presentation of numerical results

(b) Direct contact between fresh and saltwater *(a=0.5; B=40)*

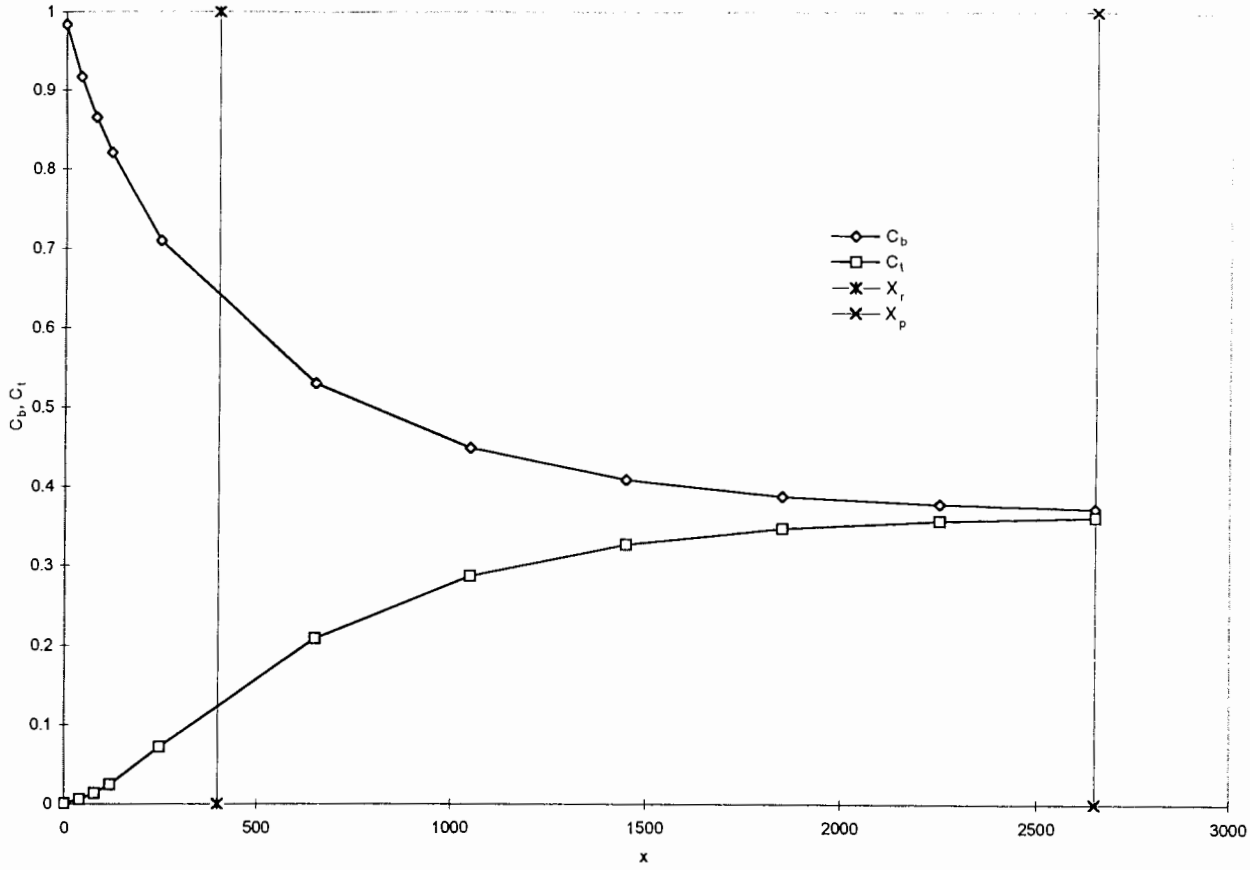

Figure 5c Variation of bottom and top salinity along the aquifer - presentation of numerical results

(c) Seepage of saltwater into the freshwater zone

($a=0.1$; $q_R=0.1$; X_e, $X_{ent}=100$; $B=24$)

We also defined another type of vertical coordinate, ζ, referring to the whole vertical cross section, as

$$\zeta = 1 - \xi \quad at \quad 0 \le y \le \delta_u \tag{22}$$

$$\zeta = 1 + \eta \quad at \quad \delta_u \le y \le B \tag{23}$$

Fig. 6 presents graphical representations of several normalized salinity profiles of c versus ζ, obtained by numerical calculations. Generally, we could identify two sections of the domain that differed with regard to the build-up of normalized salinity profiles. The first section is termed "the restructuring section". This section extends between the entrance cross section (attachment point) and x = X_r. The location X_r represents the establishment point. The second section, located downstream of the establishment point is termed "the establishment section", and extends between X_r and X_p. The location X_p represents the point of vertical uniformity of the salinity profile. Figures 6(a), (c), and (e) refer to the restructuring section, with x-values in the range $0 \le x \le X_r$. Figures 6(b), (d), and (f) refer to the establishment section, with x-values in the range $X_r \le x \le X_p$. In the restructuring section, points of c versus ζ for different cross sections did not converge to a single curve as well as in the establishment section. It seems that there is a gradual restructuring relationship between these two variables. On the other hand, in the establishment section all points converged to a single curve. Figure 6(g) shows data of simulations obtained for different types of mineralization scenarios. Data of this figure compare mineralization due to direct contact between fresh and saltwater, mineralization due to seepage of saltwater, and different values of the field parameters, i.e. a, x and B. All points displayed in Figure 6(g) converge to a single curve

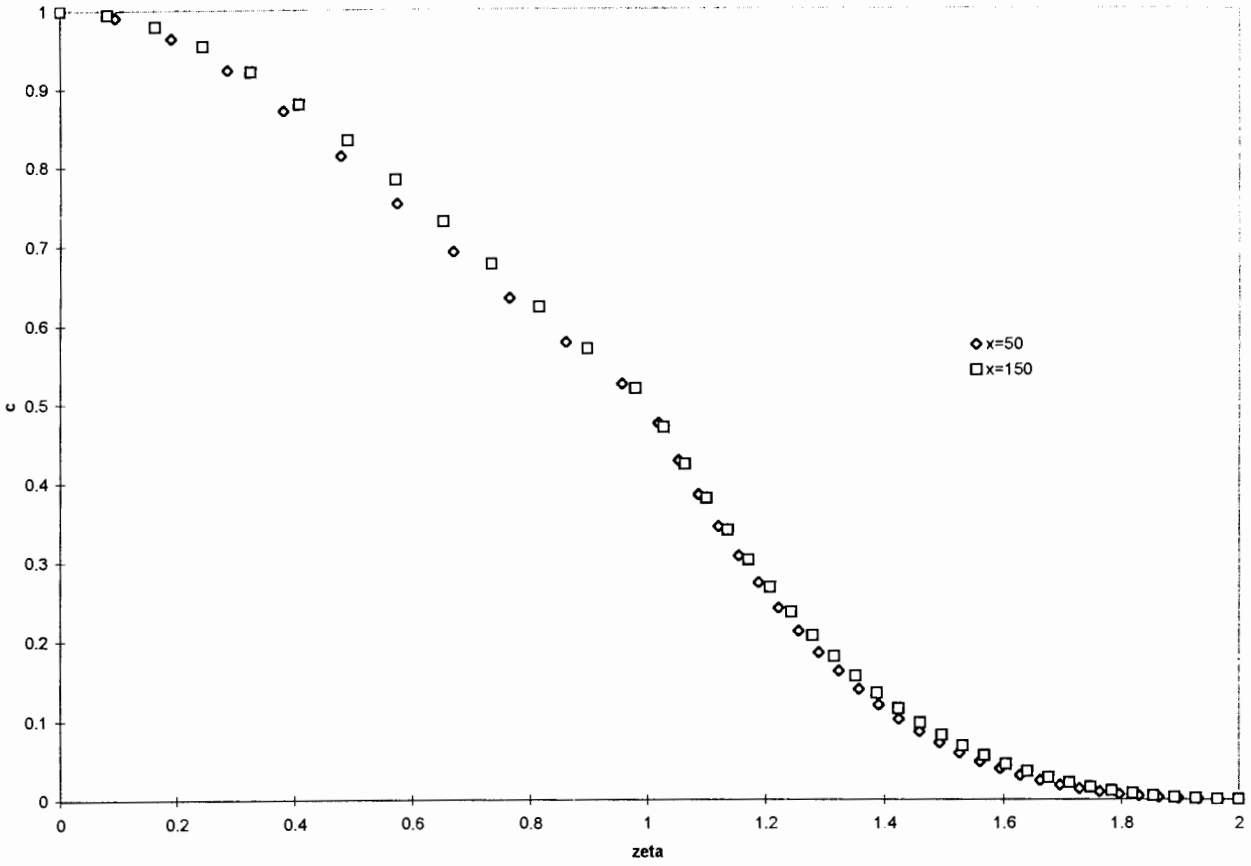

Figure 6a Normalized salinity profiles - presentation of numerical results

(a) Direct contact between fresh and saltwater

(a=0.1; B=40; $0 \leq x \leq X_r$)

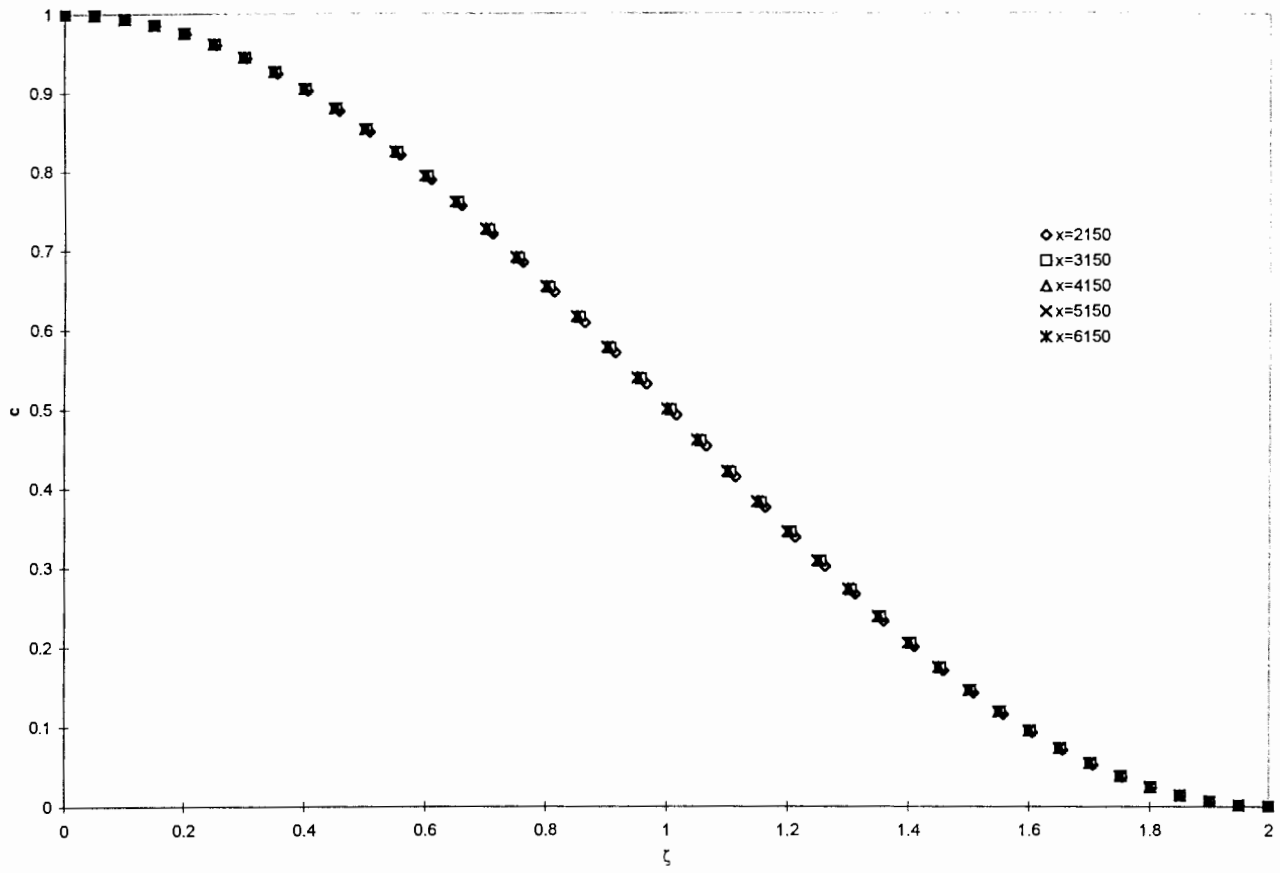

Figure 6b Normalized salinity profiles - presentation of numerical results

(b) Direct contact between fresh and saltwater

(a=0.1; B=40; $X_r \leq x \leq X_p$)

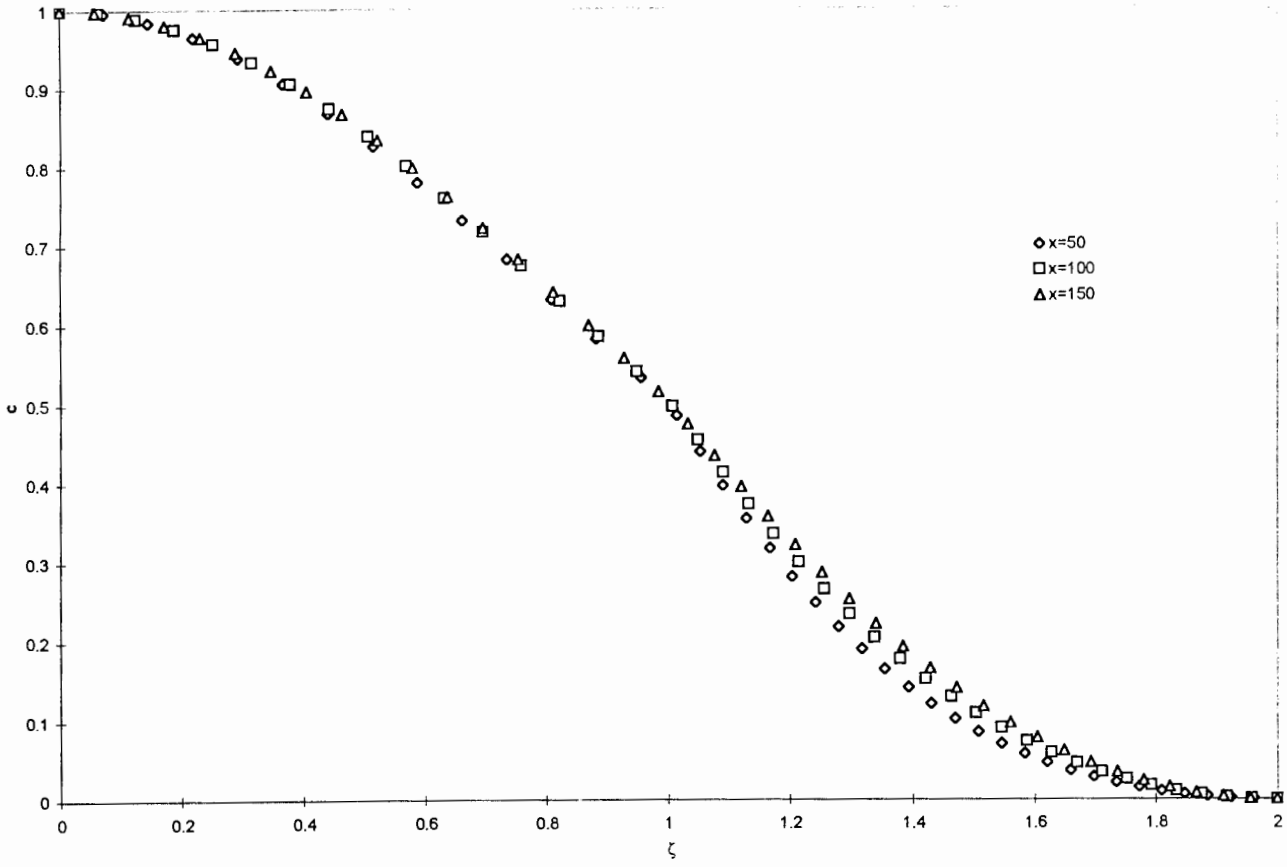

Figure 6c Normalized salinity profiles - presentation of numerical results

(c) Direct contact between fresh and saltwater

($a=0.5$; $B=40$; $0 \leq x \leq X_r$)

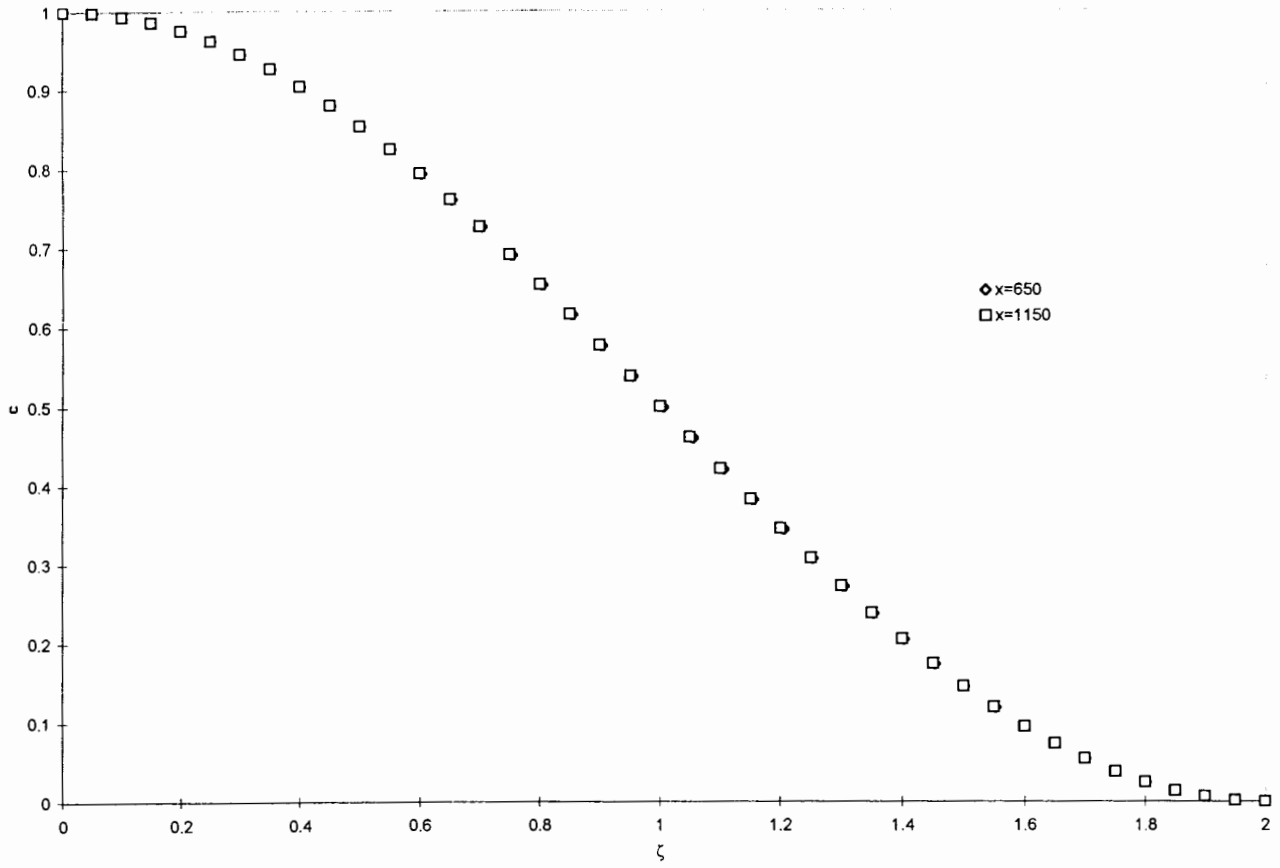

Figure 6d Normalized salinity profiles - presentation of numerical results

(d) Direct contact between fresh and saltwater

($a=0.5$; $B=40$; $X_r \leq x \leq X_p$)

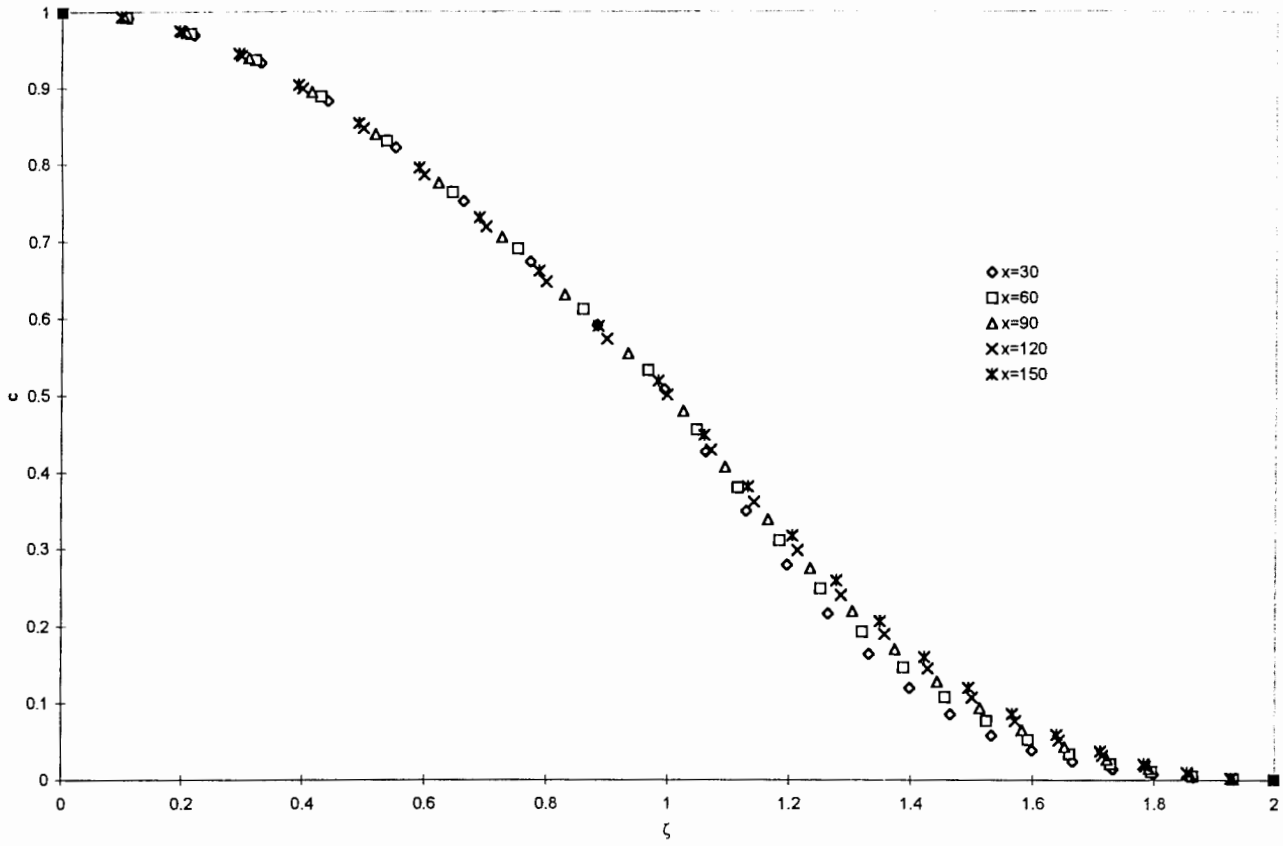

Figure 6e Normalized salinity profiles - presentation of numerical results

(e) Seepage of saltwater into the freshwater zone

($a=0.1$; $q_R=0.1$; X_e, $X_{ent}=100$; $B=24$; $0 \leq x \leq X_r$)

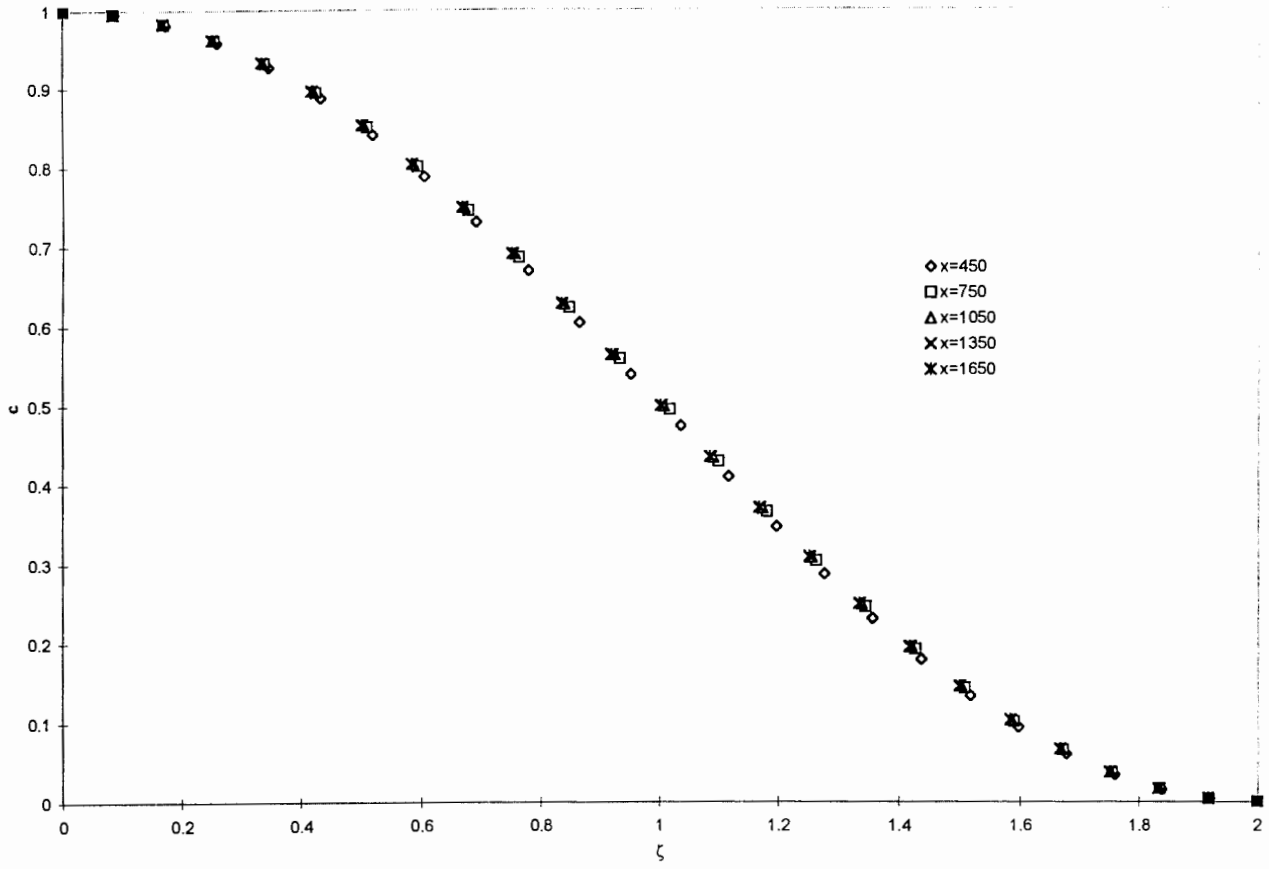

Figure 6f Normalized salinity profiles - presentation of numerical results

(f) Seepage of saltwater into the freshwater zone

($a=0.1$; $q_R=0.1$; X_e, $X_{ent}=100$; $B=24$; $X_r \leq x \leq X_p$)

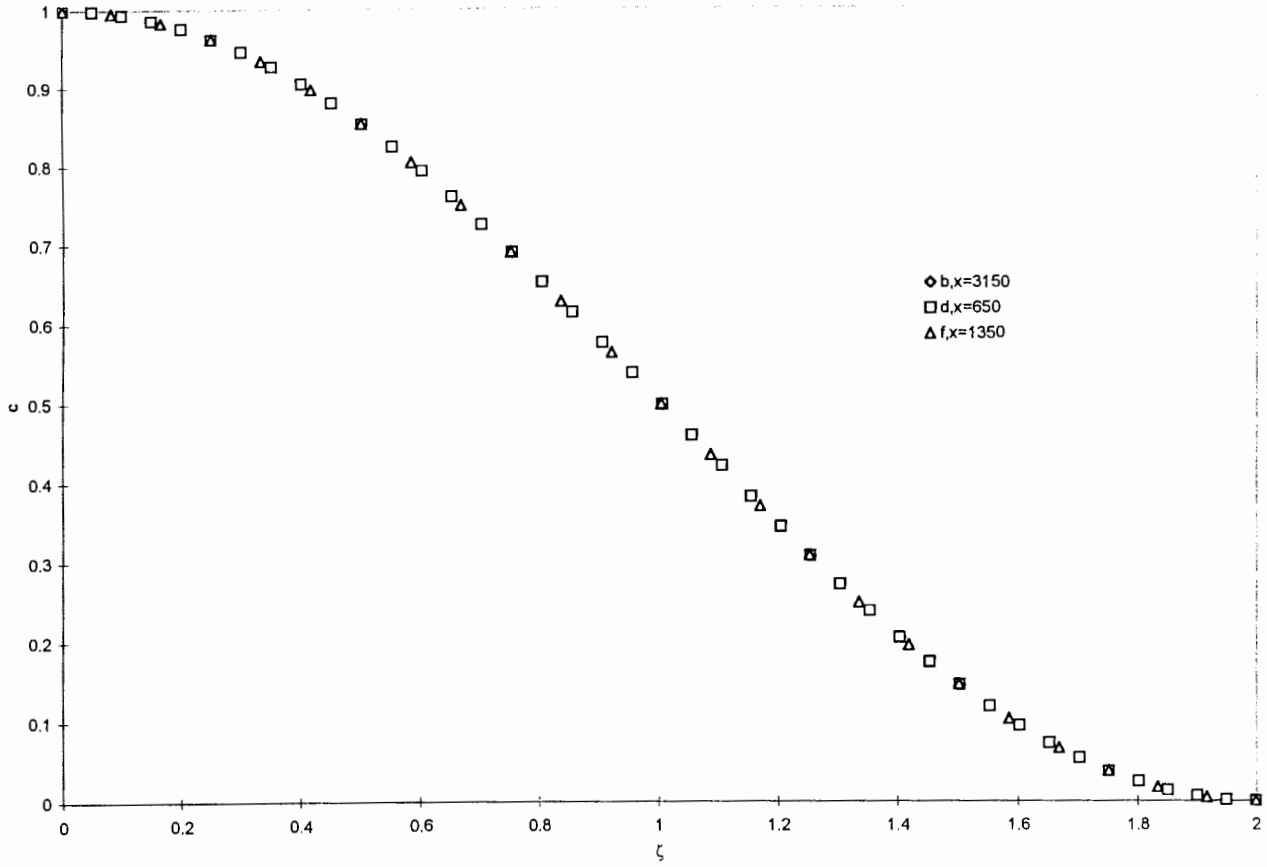

Figure 6g Normalized salinity profiles - presentation of numerical results

(g) Data of Figs. 6(b), 6(d) and 6(f)

Figure 7 displays a possible representation of the normalized salinity profiles for the two BLs built-up around the floating boundary of c = 0.5. This figure evaluates the possible representation of these profiles by the following power series expansions

$$c = 1 - 0.5(1 - \xi)^{n_1}; \qquad at \quad 0 \le y \le \delta_u \tag{24}$$

$$c = 0.5(1 - \eta)^{n_2}; \qquad at \quad \delta_u \le y \le B \tag{25}$$

Introducing eqs. (22) and (23) into eqs. (24) and (25), respectively, we obtained

$$c = 1 - 0.5\zeta^{n_1} \quad at \quad 0 \le \zeta \le 1 \quad (0 \le y \le \delta_u) \tag{26}$$

$$c = 0.5(2 - \zeta)^{n_2} \quad at \quad 1 \le \zeta \le 2 \quad (\delta_u \le y \le B) \tag{27}$$

Rearrangement of these expressions yielded

$$1 - c = 0.5\zeta^{n_1} \quad at \quad 0 \le \zeta \le 1 \tag{28}$$

$$2c = (2 - \zeta)^{n_2} \quad at \quad 1 \le \zeta \le 2 \tag{29}$$

Figure 7(a) shows normalized salinity profiles in the inner BL as represented by eq. (28). It shows that the data of Fig. 6(b) at x = 3150 converged very well to a straight line on the logarithmic scale. Figure 7(b) refers to normalized salinity profiles in the outer BL as represented by eq. (29). Again data of Fig. 6(b) at x = 3150 converged very well to a straight line on the logarithmic scale.

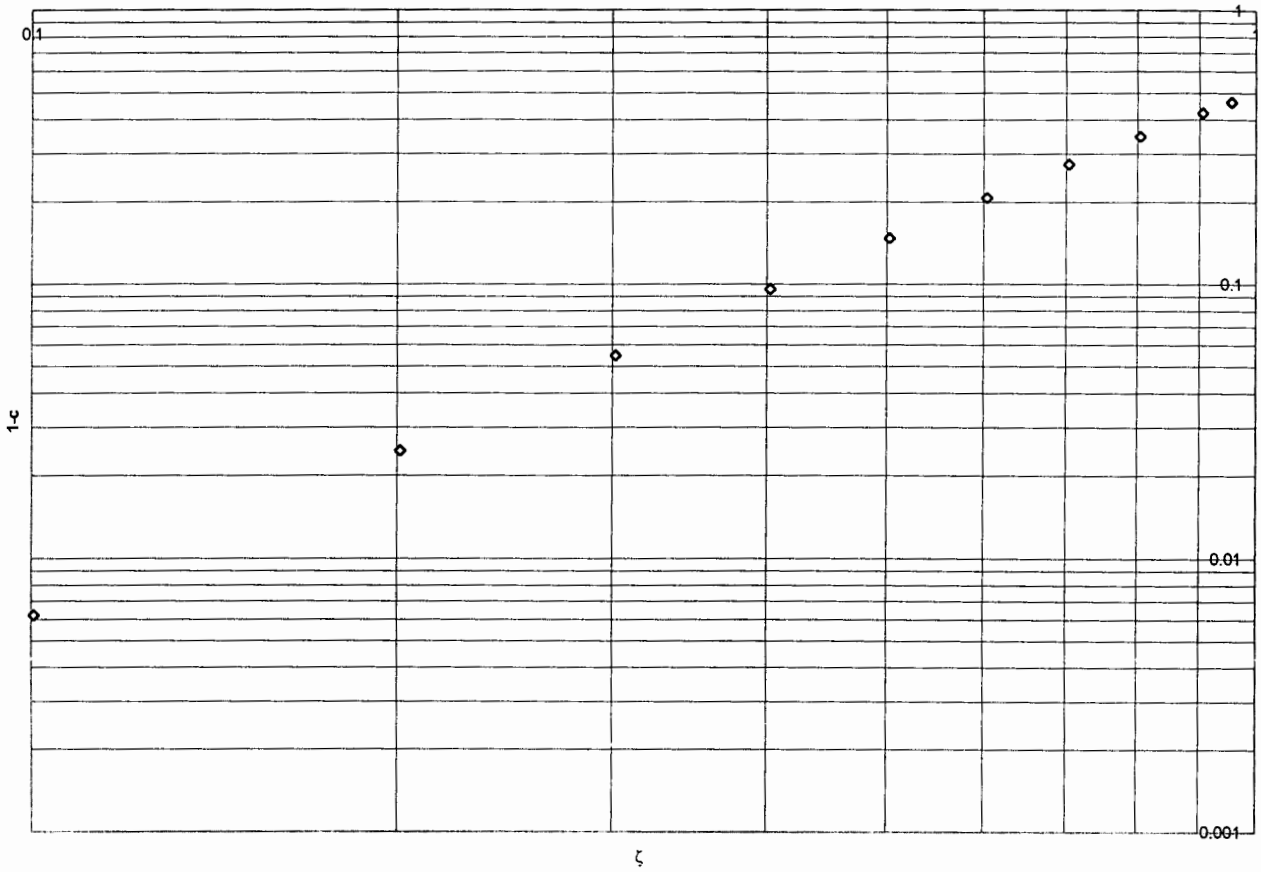

Figure 7a Adoption of appropriate power coefficients

(a) Identifying appropriate value of n_1 according to data of Fig 6(b) at *x=3150*

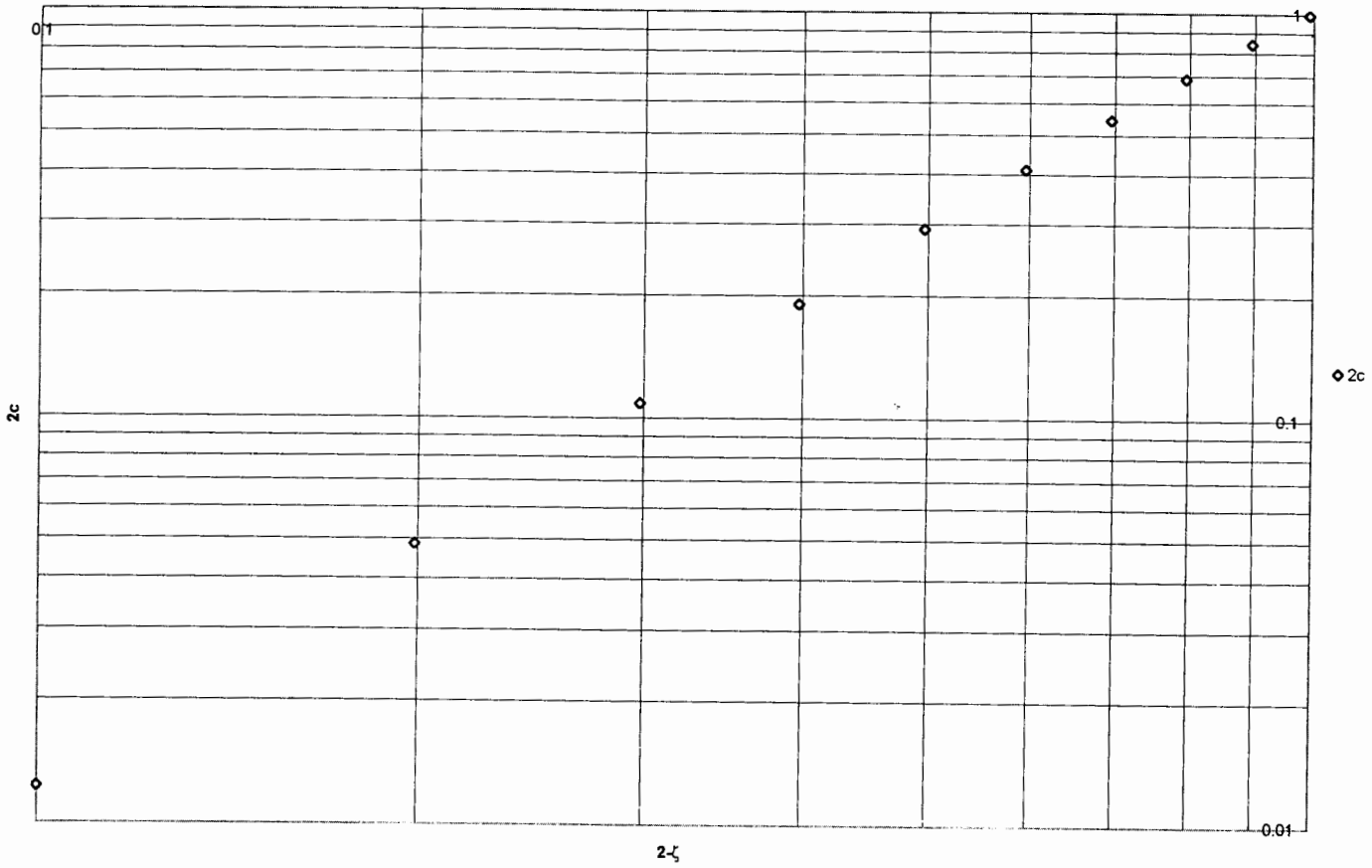

Figure 7b Adoption of appropriate power coefficients

(b) Identifying appropriate value of n_2 according to data of Fig 6(b) at x=3150

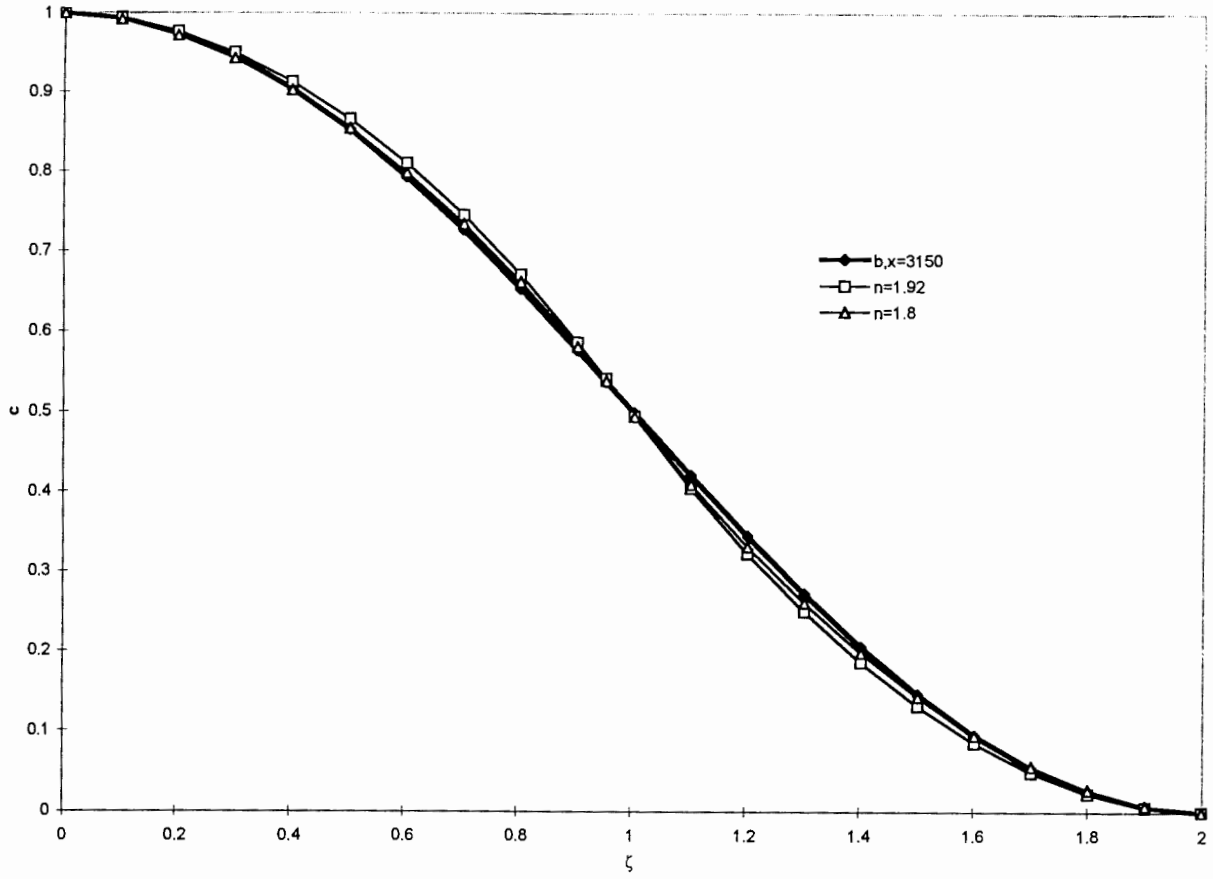

Figure 7c Adoption of appropriate power coefficients

(c) Comparison between salinity profile data and series expansions

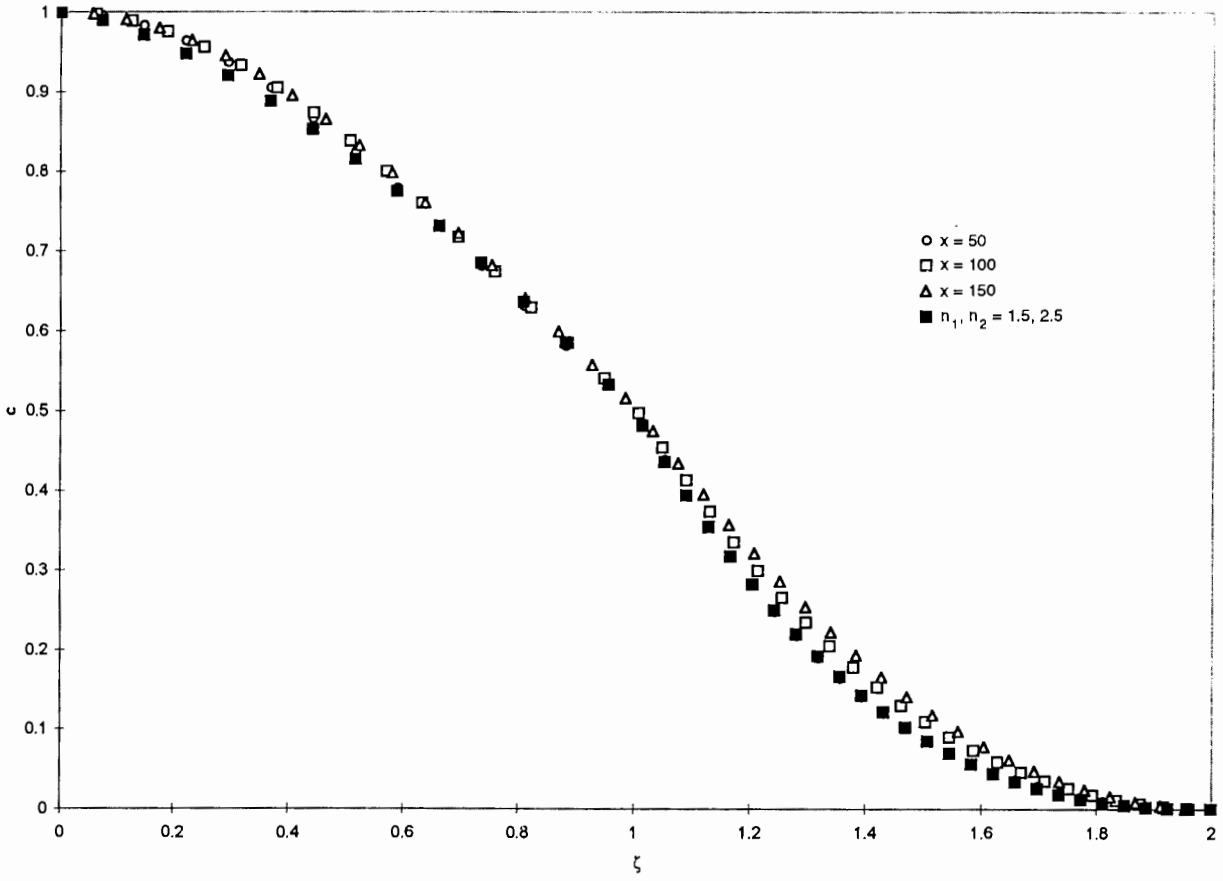

Figure 7d Adoption of appropriate power coefficients

(d) Comparison between data of Fig. 6(c) and power series expansion

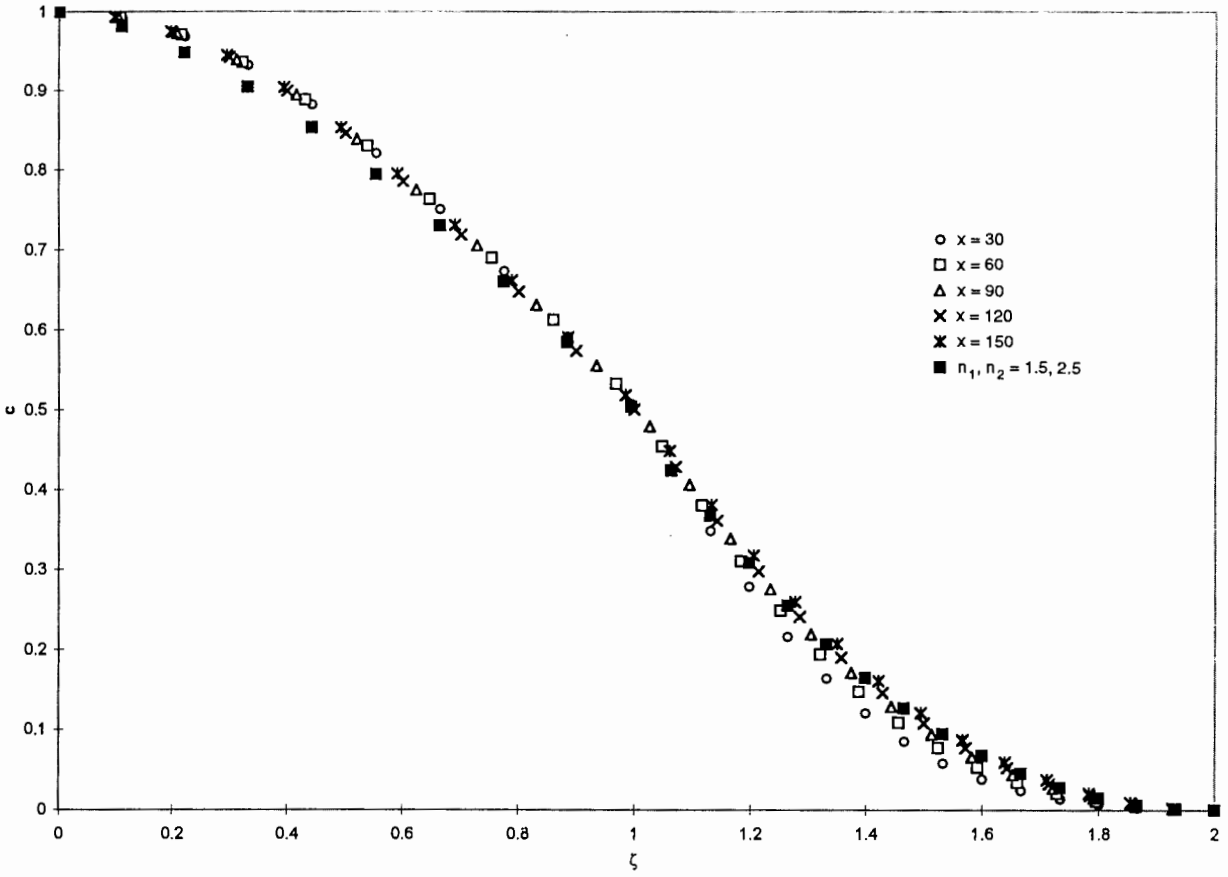

Figure 7e Adoption of appropriate power coefficients

(e) Comparison between data of Fig. 6(e) and power series expansion

Power regression analysis of the data given in Fig. 7(a) provided, with a correlation factor of 0.9997, the following expression for the normalized salinity profiles in the inner BL:

$$1 - c = 0.53\zeta^{1.92} \tag{30}$$

Power regression analysis of the data given in Fig. 7(b) provided, with a correlation factor of 0.9996, the following expression for the normalized salinity profiles in the outer BL:

$$2c = 1.076(2 - \zeta)^{1.92} \tag{31}$$

We used coefficients of 0.5 rather than 0.53 in eq. (30), and 1.0 rather than 1.076 in eq. (31). Under such conditions calculated values of n_1 and n_2 by least square deviations yielded $n_1 = n_2 = 1.9$. However visual estimates based on Fig. 7(c) suggested using $n_1 = n_2 = 1.8$.

At the downstream end of the restructuring section, i.e. at the establishment point $x = X_r$, values of n_1 and n_2 approach their value in the establishment section. At the upstream end of this section, i.e. the attachment point, which is the entrance cross section, the normalized salinity distribution is that of an infinite (vertical) aquifer. Therefore, in this section, similarity of the normalized salinity profiles cannot be perfect. According to least square deviations and some visual observations of numerical experiments based on the data of Figs. (6d) and 6(e) and represented in Figs 7(d) and 7(e), respectively, we adopted power coefficient values of $n_1 = 1.5$ and $n_2 = 2.5$.

Employment of the top specified boundary layer (TSBL) approach

The numerical experiments, discussed in the preceding section, indicate that in the establishment section, it is possible to identify inner and outer BLs. Each of these BLs occupies about half of the thickness of the aquifer. On the other hand, in the restructuring section, it was possible to identify such BLs only approximately. This approximation is quite good, but not in perfect agreement with the data obtained by the numerical

simulations. Therefore, predictions based on a BL approach can be expected to fit better to the establishment section than the restructuring section.

The objective of developing a BL approach was to obtain analytical expressions for the characterization of salinity penetration into the aquifer. Such an approach was based on the adoption of some acceptable conceptual modeling leading to simplified calculations which could provide a reasonable approximation of transport phenomena in the evaluated domain. In the following paragraphs, use of this basic approach to develop expressions representing the expansion of the inner BL and variation of salinity distribution in the evaluated domain is described. At the attachment point (the entrance cross section) salt concentration at the top of the aquifer is about one tenth of a percent of its value at the bottom of the aquifer, and the thickness of the region of interest (ROI) is smaller than the thickness of the aquifer. Under such conditions, according to the TSBL approach, we can consider that the aquifer thickness was infinite upstream of the entrance cross section.

Generally, the vertical salinity gradient can lead to two simultaneous phenomena: (a) expansion of the inner BL, and (b) salinity transfer from the inner BL into the outer BL. The inner BL maximum thickness is $B/2$, where B is the thickness of the aquifer. The numerical experiments showed that in the so-called restructuring section, the inner BL varies significantly with x. However, in the so-called establishment section, the inner BL is close to its final value, and its vertical expansion along the length of the aquifer is almost negligible. Therefore, we assume that in the restructuring section the vertical salinity gradient results only in the expansion of the inner BL, and there is no salinity transfer between the inner and outer BLs. At the establishment point, which is located at the downstream end of the restructuring section, the inner BL occupies approximately half of the aquifer thickness. In the establishment section, located downstream of the establishment point, the vertical salinity gradient results solely in transfer of salinity from the inner BL into the outer BL, with no more expansion of the inner BL.

According to eqs. (14), (20) and (24), salinity distribution in the inner BL is given by

$$\frac{C-C_t}{C_b-C_t}=1-0.5(1-\xi)^{n_1};\quad where\quad \xi=\frac{\delta_u-y}{\delta_u};\quad at\quad 0\le y\le \delta_u \tag{32}$$

According to eqs.(14), (21) and (25), salinity distribution in the outer BL is given by

$$\frac{C-C_t}{C_b-C_t}=0.5(1-\eta)^{n_2};\quad where\quad \eta=\frac{y-\delta_u}{B-\delta_u};\quad at\quad \delta_u\le y\le B \tag{33}$$

We assumed that in the restructuring section there is no salinity transfer between the inner and outer BLs. Therefore, by integrating the salinity profiles in both layers we can obtain for the restructuring section

$$C_b=\frac{C_{b0}}{2(n_1+0.5)(n_2+0.5)-0.5}\left[2(n_1+0.5)(n_2+0.5)\frac{\delta_{u0}}{\delta_u}-0.5\frac{B-\delta_{u0}}{B-\delta_u}\right] \tag{34}$$

$$C_t=\frac{C_{b0}(n_1+0.5)}{2(n_1+0.5)(n_2+0.5)-0.5}\left[\frac{B-\delta_{u0}}{B-\delta_u}-\frac{\delta_{u0}}{\delta_u}\right] \tag{35}$$

where C_{b0} and δ_{u0} are values of C_b and δ_u at $x = 0$, respectively.

Fig. 8 presents a schematic description of the spatial variation of salinity distribution and geometry of the inner and outer BLs over a small space interval. Applying the Lagrangian approach, spatial variations shown in Fig. 8 can be considered as a combination of spatial and temporal changes. We assume that the rate of expansion of the inner BL is related to the salinity gradients and salinity flux in the domain, and that the salinity flux associated with the rate of expansion of the inner BL is related to the average salinity diffusive flux. Therefore, by applying the approach illustrated in Fig. 8 to these assumptions and using the principle of mass conservation, we obtain:

$$0.5(C_b + C_t)\frac{d\delta_u}{dt} = -\gamma a\left(\frac{\partial C}{\partial y}\right)_{y=\delta_u} \tag{36}$$

where γ is a coefficient, which should be determined by best fit of the model.

By introducing eq. (32) into eq. (36), we obtain:

$$\frac{C_b + C_t}{C_b - C_t}\frac{d\delta_u}{dt} = \gamma\frac{an_1}{\delta_u} \tag{37}$$

By applying eqs. (34) and (35), we obtain:

$$\frac{C_b + C_t}{C_b - C_t} = \frac{2n_2(n_1 + 0.5)\dfrac{\delta_{u0}}{\delta_u} + n_1\dfrac{B - \delta_{u0}}{B - \delta_u}}{2(n_1 + 0.5)(n_2 + 0.5)\dfrac{\delta_{u0}}{\delta_u} - (n_1 + 1)\dfrac{B - \delta_{u0}}{B - \delta_u}} \tag{38}$$

We introduced eq. (38) into eq.(37), separated variables, and directly integrated the equation under the condition that the value of the inner boundary layer is δ_{u0} at $x = 0$, to obtain:

$$\gamma\frac{an_1 x}{B^2} = -\beta_1\left(\frac{\delta_u}{B} - \frac{\delta_{u0}}{B}\right) + \beta_2\left[\left(\frac{\delta_u}{B}\right)^2 - \left(\frac{\delta_{u0}}{B}\right)^2\right] - \beta_3\ln\left[\frac{\beta_4 - \beta_5\left(\dfrac{\delta_u}{B}\right)}{\beta_4 - \beta_5\left(\dfrac{\delta_{u0}}{B}\right)}\right] \tag{39}$$

where β_i (i = 1,...5) are coefficients given by:

$$\beta_1 = \frac{2(n_1 + 0.5)\left(1 - \dfrac{\delta_{u0}}{B}\right)\left(\dfrac{\delta_{u0}}{B}\right)[n_2(n_1 + 1) + n_1(n_2 + 0.5)]}{\left[2(n_1 + 0.5)(n_2 + 0.5)\left(\dfrac{\delta_{u0}}{B}\right) + (n_1 + 1)\left(1 - \dfrac{\delta_{u0}}{B}\right)\right]^2} \tag{40a}$$

$$\beta_2 = \frac{2n_2(n_1+0.5)\left(\frac{\delta_{u0}}{B}\right) - n_1\left(1-\frac{\delta_{u0}}{B}\right)}{2\left[2(n_1+0.5)(n_2+0.5)\left(\frac{\delta_{u0}}{B}\right)+(n_1+1)\left(1-\frac{\delta_{u0}}{B}\right)\right]} \tag{40b}$$

$$\beta_3 = \frac{4(n_1+0.5)^2(n_2+0.5)\left(1-\frac{\delta_{u0}}{B}\right)\left(\frac{\delta_{u0}}{B}\right)^2[n_2(n_1+1)+n_1(n_2+0.5)]}{\left[2(n_1+0.5)(n_2+0.5)\left(\frac{\delta_{u0}}{B}\right)+(n_1+1)\left(1-\frac{\delta_{u0}}{B}\right)\right]^3} \tag{40c}$$

$$\beta_4 = 2(n_1+0.5)(n_2+0.5)\left(\frac{\delta_{u0}}{B}\right) \tag{40d}$$

$$\beta_5 = 2(n_1+0.5)(n_2+0.5)\left(\frac{\delta_{u0}}{B}\right)+(n_1+1)\left(1-\frac{\delta_{u0}}{B}\right) \tag{40e}$$

Equation (39) implies that at $\delta_u = B/2$ the restructuring section ends and $x = X_r$. Therefore:

$$X_r = \frac{B^2}{\gamma a n_1}\left\{-\beta_1\left[\left(\frac{1}{2}\right)-\left(\frac{\delta_{u0}}{B}\right)\right]+\beta_2\left[\left(\frac{1}{2}\right)^2-\left(\frac{\delta_{u0}}{B}\right)^2\right]+\beta_3\ln\left[\frac{\beta_4-\beta_5\left(\frac{1}{2}\right)}{\beta_4-\beta_5\left(\frac{\delta_{u0}}{B}\right)}\right]\right\} \tag{41}$$

As indicated by the numerical experiments, the value of the coefficient γ is about 2.54.

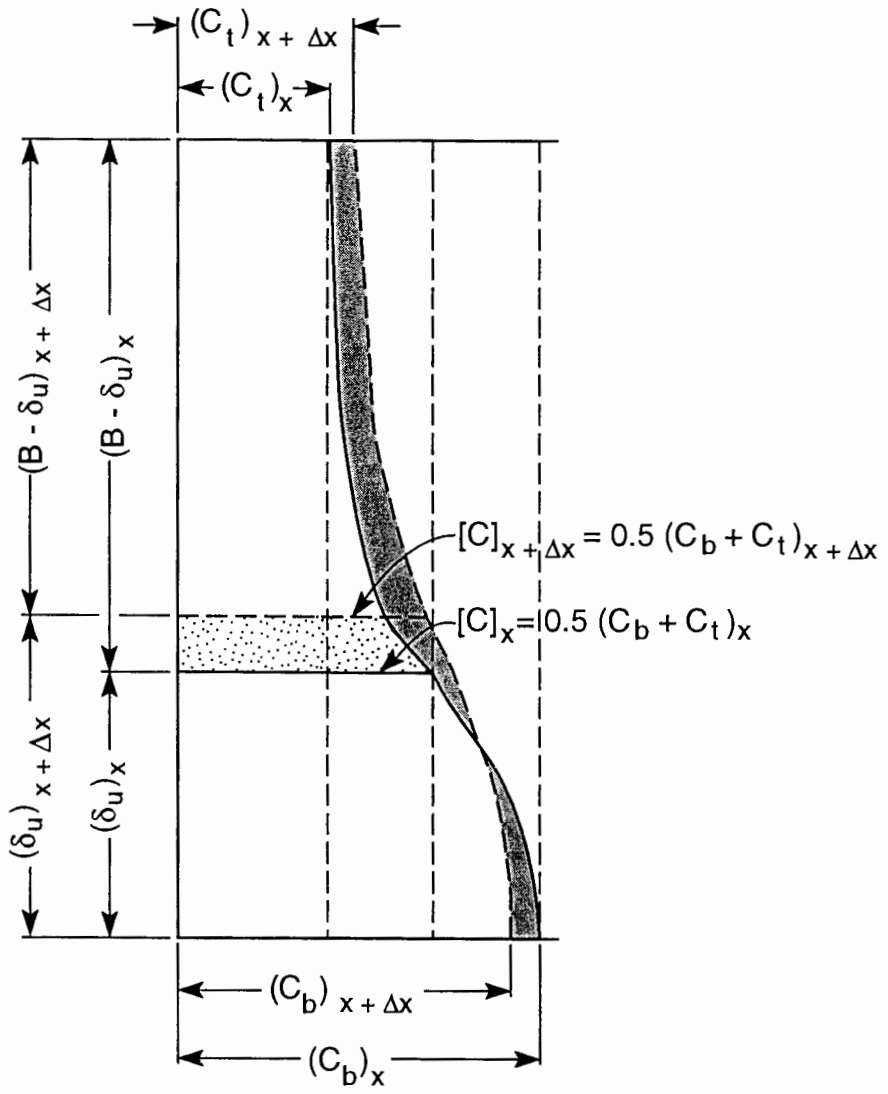

Figure 8 Schematic of the inner boundary layer expansion in the restructuring section, showing how changes in salinity distribution are ascribed to shifts in BL dimensions.

The system of eqs. (32) - (35) and (39) completely determines the variation of the inner BL thickness and salinity distribution along the aquifer in the restructuring section.

Use of the TSBL method requires some salinity profile adjustments at the attachment point (the entrance cross section), and at the establishment point (the interface between the restructuring and establishment sections). These adjustments originate from the mass conservation principle. At the entrance cross section, the conservation of mass yields:

$$\left[\int_0^B C dy\right]_{ent-} = \left[\int_0^{\delta_u} C dy + \int_{\delta_u}^B C dy\right]_{ent+} \tag{42}$$

where *ent+* and *ent-* are subscripts referring to the right and left hand sides of the entrance cross section, respectively. We assume that C_t vanishes at both sides of the entrance cross section, and introduce eqs. (32) and (33) into eq. (44) to obtain:

$$\frac{1}{B}\left[\int_0^B C dy\right]_{ent-} = C_{b0}\left[\frac{0.5}{n_2+1} + \frac{\delta_{u0}}{B}\left(\frac{n_1+0.5}{n_1+1} - \frac{0.5}{n_2+1}\right)\right] \tag{43}$$

where C_{b0} and δ_{u0} are values of C_b and δ_u at the right hand side of the entrance cross section.

In order to satisfy eq. (43) the entrance value of C_{b0} or δ_{u0} must be modified. It is reasonable to modify the value of C_{b0}, as the bottom boundary condition of vanishing salinity flux primarily controls this bottom parameter. However, eq. (43) provides the basis for adjustment of values of both parameters, subject to the constraint that the maximum value of C_{b0} is unity. If eq. (43) implies that the value of C_{b0} should exceed this limit, then adjustment of δ_{u0} is also necessary.

At the establishment point, which represents the interface between the restructuring and establishment sections, some minor adjustments of values of C_b and C_t,

are also required by the principle of mass conservation. Integrating the salinity profiles at both sides of that point yields:

$$[C_b + C_t]_{r+} = \left[C_b \left(\frac{n_1 + 0.5}{n_1 + 1} + \frac{0.5}{n_2 + 1} \right) + C_t \left(\frac{n_2 + 0.5}{n_2 + 1} + \frac{0.5}{n_1 + 1} \right) \right]_{r-} \tag{44}$$

where $r+$ and $r-$ are subscripts referring to right and left hand side of the establishment point at $x = X_r$, respectively.

From eq. (44) it can be inferred that:

$$[C_b]_{r+} = \left(\frac{n_1 + 0.5}{n_1 + 1} + \frac{0.5}{n_2 + 1} \right) [C_b]_{r-} \tag{45}$$

$$[C_t]_{r+} = \left(\frac{n_2 + 0.5}{n_2 + 1} + \frac{0.5}{n_1 + 1} \right) [C_t]_{r-} \tag{46}$$

Figure 9 shows an example comparing the results of numerical simulations with those obtained by the TSBL approach. Data for the restructuring section in Fig. 9(a) shows variations of the inner BL thickness along the aquifer. Fig. 9(b) shows changes in values of C_b and C_t along the aquifer.

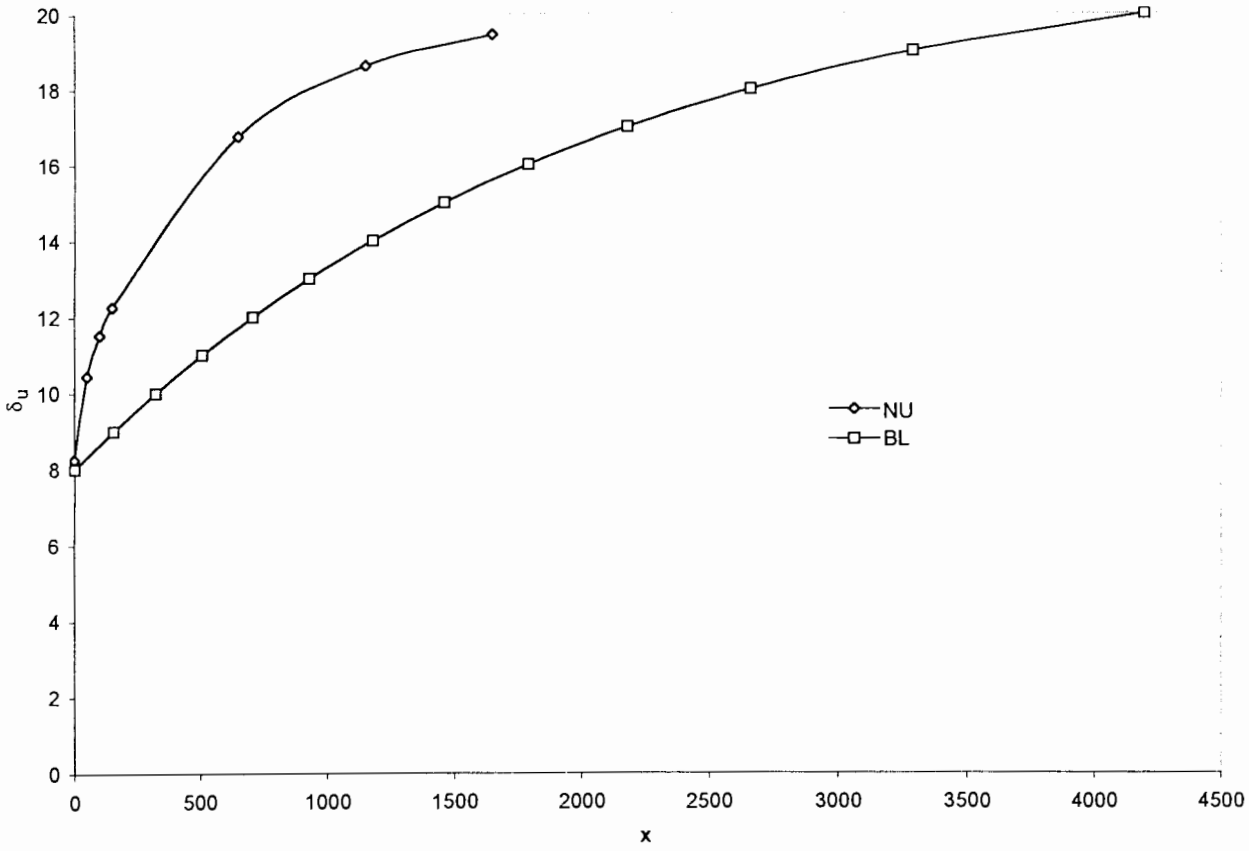

Figure 9a Comparison between the TSBL prediction (BL) referring to the restructuring section and numerical results (NU) for direct contact between fresh and saltwater, with *($a=0.1$; $B=40$; $0 \leq x \leq X_r$)*

(a) Variation of the inner boundary layer thickness along the aquifer

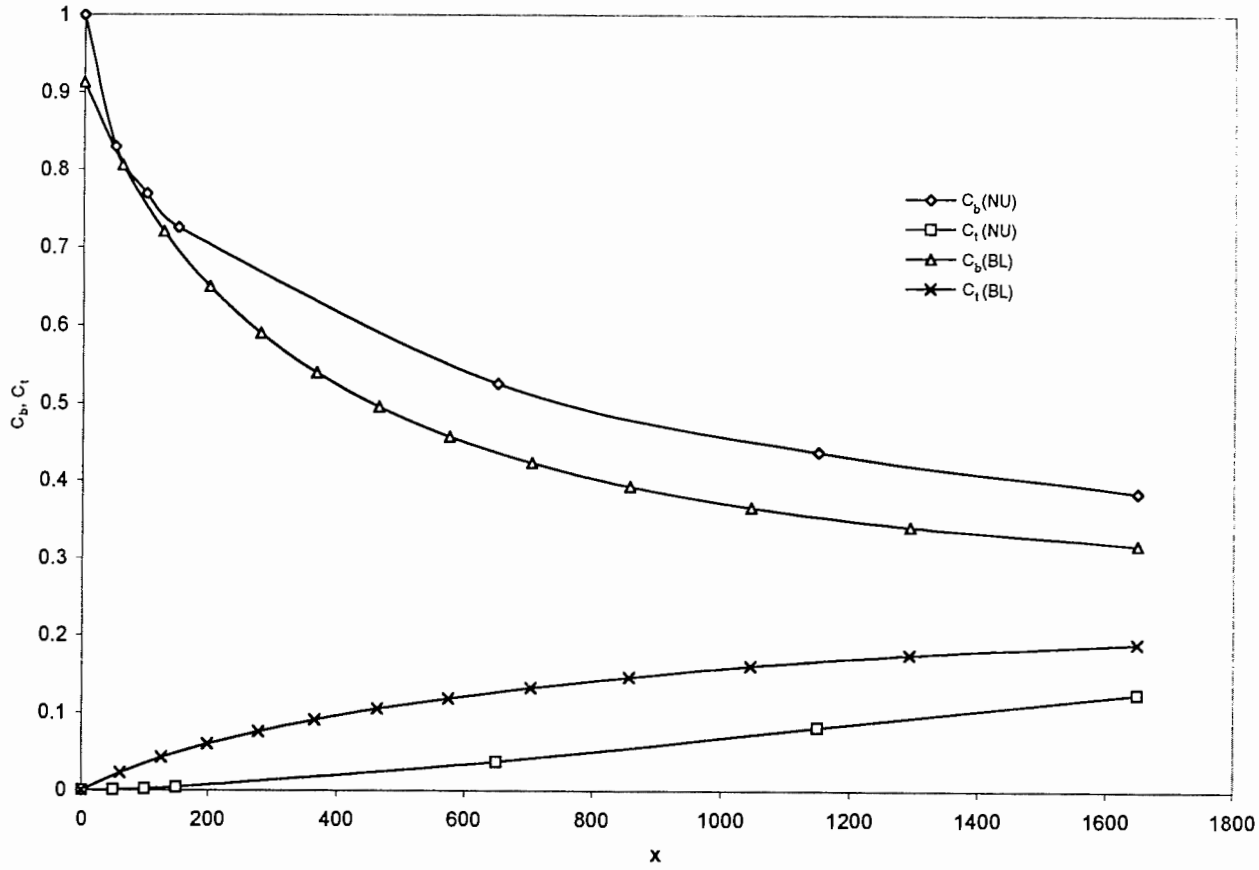

Figure 9b Comparison between the TSBL prediction (BL) referring to the restructuring section and numerical results (NU) for direct contact between fresh and saltwater, with *(a=0.1; B=40; $0 \leq x \leq X_r$)*

(b) Variation of bottom and top salinity along the aquifer

Figure 9 shows differences between predictions supplied by the TSBL method developed in this study and the numerical results. It should be noted that this figure refers to the entrance salinity profile given in Fig. 3(a), which is substantially different from salinity profiles existing downstream of the entrance cross section. Therefore, we modified the value of C_{b0} by applying eq. (43). As shown in the specific example of Fig. 9(b), the value of this parameter is 0.9 instead of 1. Figure 9 implies that our assumption of no transfer of salinity between the inner and outer BLs provides a well-defined value for X_r, in which the inner BL occupied half of the aquifer thickness. At that value of x, the numerical calculations indicate that the inner BL occupies about 49 percent of the aquifer thickness. In the particular example given by Fig. 9, we have obtained X_r = 1600. The numerical calculations show that the transition from the restructuring to the establishment section is moderate and extends along a significant length of the aquifer. Since the major practical use of the present study is probably the initial evaluation of horizontal penetration of salinity into an aquifer subject to mineralization, the approximate values represented in Fig. 9 are sufficiently accurate for practical purposes. In most cases, errors introduced by this assumption would be no larger than uncertainties in knowledge of the aquifer and groundwater flow characteristics.

Fig. 10 represents schematics of salinity transfer in the establishment section. It depicts the transfer of salinity from the inner into the outer BL over a small spatial interval. The aquifer thickness is occupied by the inner and outer BLs, whose thicknesses are identical, and a salinity body is transferred from the inner into the outer BL. The graphical representation of this salinity body has almost the shape of a triangle whose base is equal to half of the rate of change of the difference between C_b and C_t, and whose height is $B/2$. If we assume that the rate of transfer of this salinity body is proportional to the salinity gradient at the centerline of the aquifer cross section, then:

$$\frac{1}{4}\frac{d}{dt}[\delta_u (C_b - C_t)] = \alpha a \left(\frac{\partial C}{\partial y}\right)_{y=B/2} \tag{47}$$

where α is a coefficient that should be smaller than one.

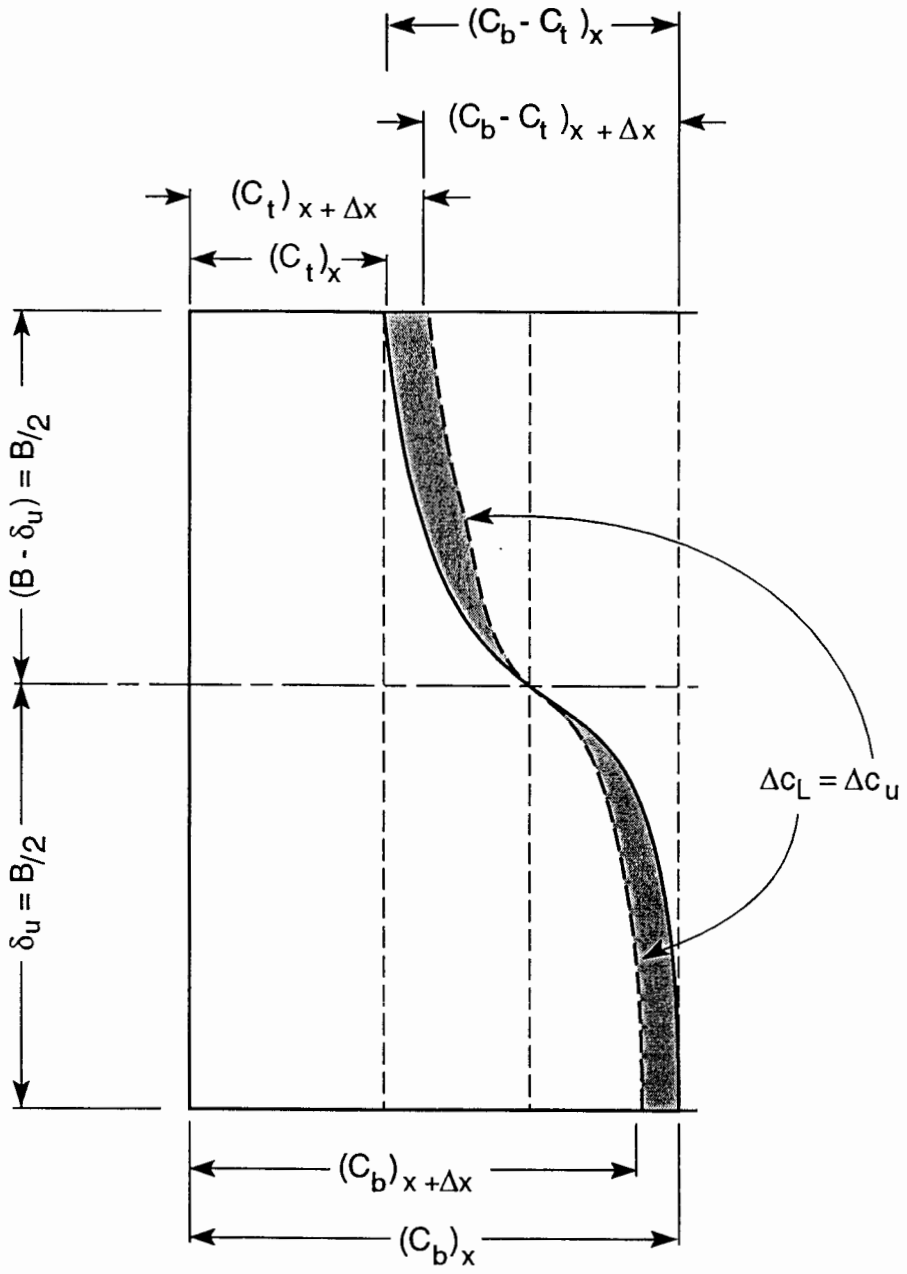

Figure 10 Schematic of salinity transfer from the inner into the outer boundary layer in the establishment section.

Considering that $\delta_u = B/2$ and introducing the appropriate expression for the salinity gradient at the aquifer centerline, we obtain:

$$\frac{d}{dt}\left[\ln\left(C_b - C_t\right)\right] = -\alpha\frac{8an}{B^2} \tag{48}$$

where $n = n_1 = n_2$.

By direct integration of eq. (48), and reference to boundary conditions at the point of establishment, where $x = X_r$, we obtain:

$$\ln\left[\frac{C_b - C_t}{\left(C_b - C_t\right)_r}\right] = -\alpha\frac{8an}{B^2}\left(x - X_r\right) \tag{49}$$

where subscript r refers to values occurring at the right hand side of the establishment point, located between the restructuring and establishment sections.

The value of X_p is defined as the place at which the difference between C_b and C_t is less than 0.01. Therefore, eq. (49) implies

$$X_p - X_r = \frac{B^2}{8\alpha an}\ln\left[100\left(C_b - C_t\right)_r\right] \tag{50}$$

Owing to the identical thickness of both BLs, as well as identical power coefficient characterizing the salinity profiles in both boundary layers, the conservation of mass principle yields

$$C_b + C_t = \left(C_b + C_t\right)_r \tag{51}$$

By applying eqs. (49) and (51) we obtain

$$C_b = \frac{1}{2}\left[(C_b + C_t)_r + (C_b - C_t)_r F\right] \tag{52}$$

$$C_t = \frac{1}{2}\left[(C_b + C_t)_r - (C_b - C_t)_r F\right] \tag{53}$$

where

$$F = \exp\left[-\alpha \frac{8an}{B^2}(x - X_r)\right] \tag{54}$$

As shown in Fig. 9(b), the value of (C_b - C_t) at X_r, as predicted by the TSBL approach, is somewhat smaller than that obtained by numerical simulations. Therefore, the expected value of α should be considerably smaller than one. The various numerical simulations performed in the preliminary tests suggest that:

$$\alpha = 0.60 \tag{55}$$

It should be noted that although eqs. (41) and (50) are based on different effects originating from vertical salinity gradients in the aquifer cross section, values of X_r, as well as the extent of the establishment section, are approximately proportional to B^2/a.

Fig. 11 shows two complete examples in which we compared results of the TSBL method with those obtained by numerical solution of the equation of salinity transport. Values of the inner BL thickness and values of salinity at the bottom and top of the aquifer obtained by both methods are given for both restructuring and establishment sections. Figs. 11(a) and 11(b) refer to direct contact between fresh and saltwater and a comparatively thick aquifer. Figs. 11(c) and 11(d) refer to seepage of saltwater into a comparatively thin freshwater aquifer. In both cases, the results of the TSBL approach are in quite good agreement with the numerical results.

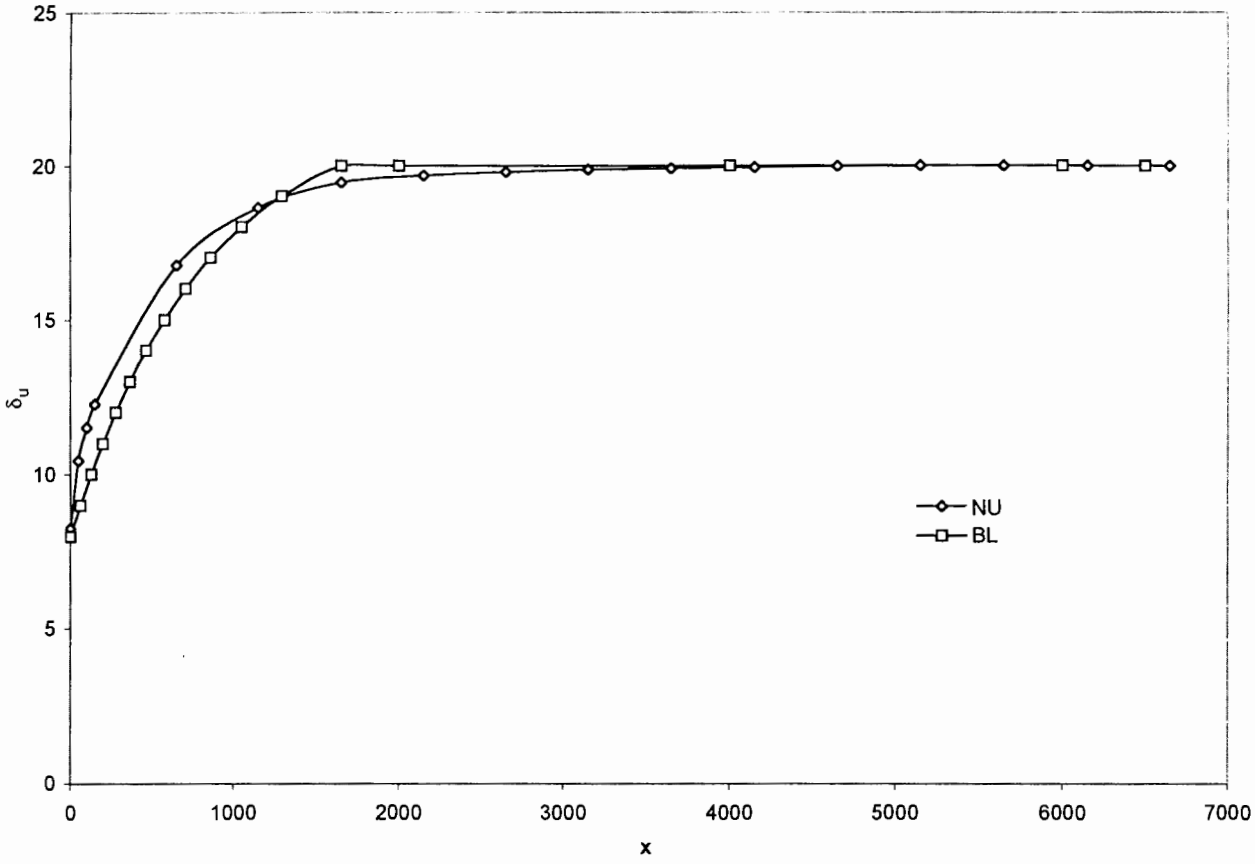

Figure 11a Comparison between the TSBL predictions (BL) referring to the restructuring and establishment sections and numerical results (NU).

(a) Variation of the inner boundary layer thickness along the aquifer. Direct contact between fresh and saltwater (a=0.1; B=40; $0 \leq x \leq X_p$)

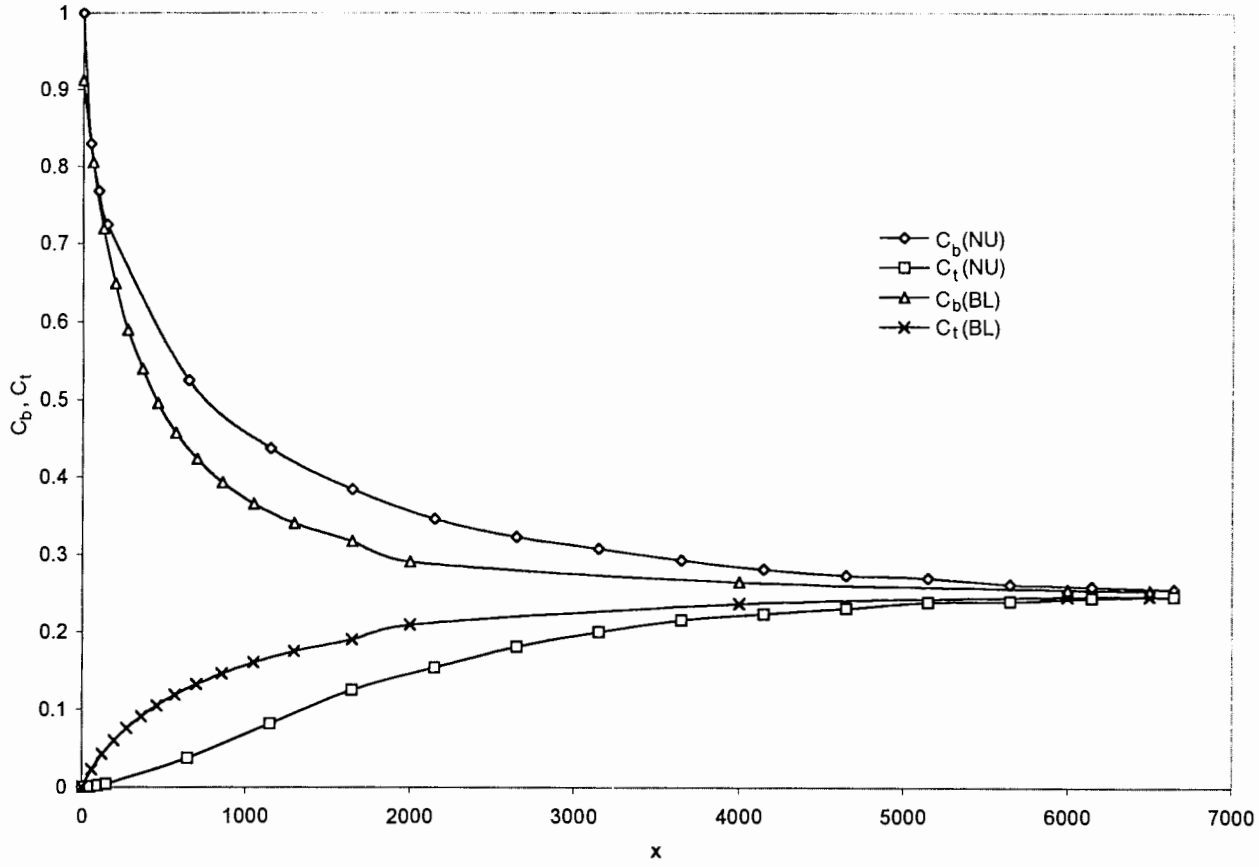

Figure 11b Comparison between the TSBL predictions (BL) referring to the restructuring and establishment sections and numerical results (NU).

(b) Variation of bottom and top salinity along the aquifer
Direct contact between fresh and saltwater (a=0.1; B=40; $0 \leq x \leq X_p$)

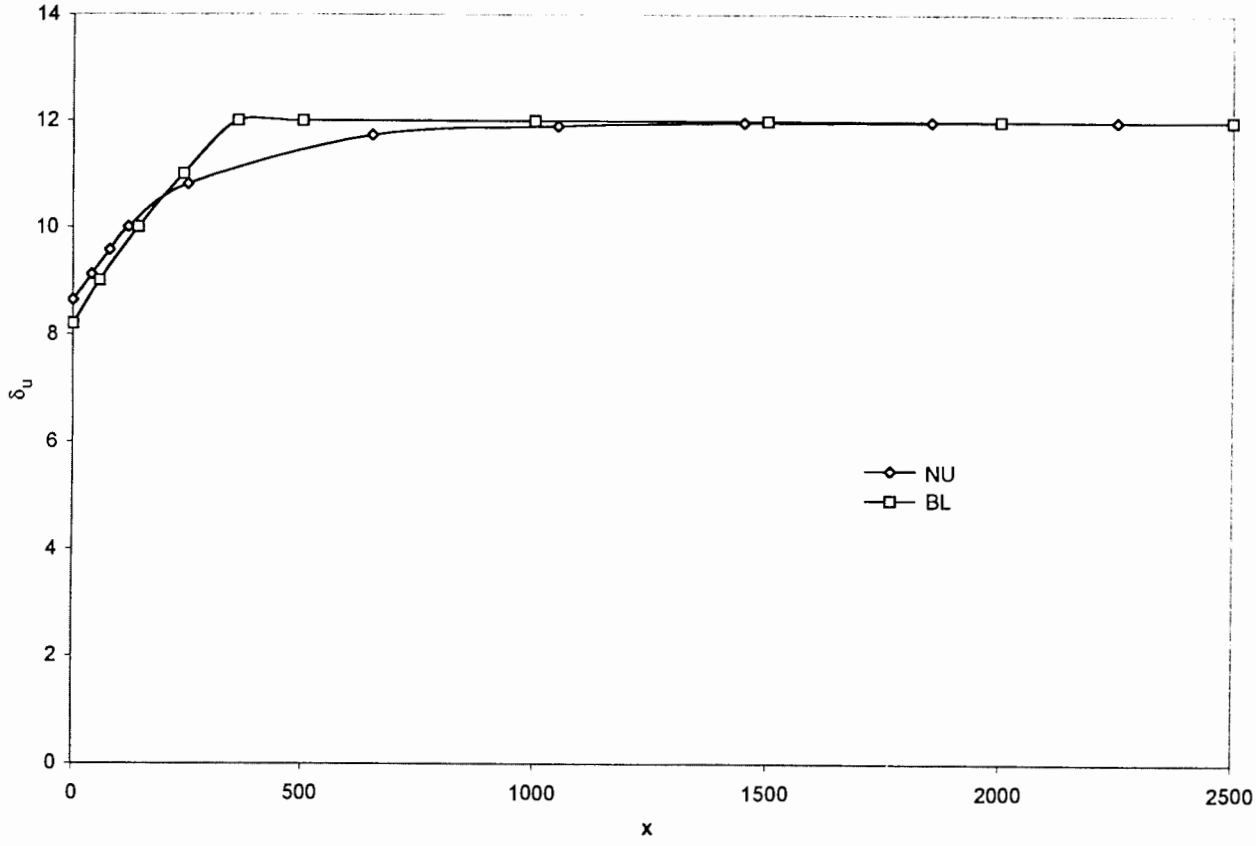

Figure 11c Comparison between the TSBL predictions (BL) referring to the restructuring and establishment sections and numerical results (NU).

(c) Variation of the inner boundary layer thickness along the aquifer
Seepage of saltwater into the freshwater zone

(a=0.1; q_R =0.1; X_e, X_{ent} = 100 ; B=24; $0 \leq x \leq X_p$)

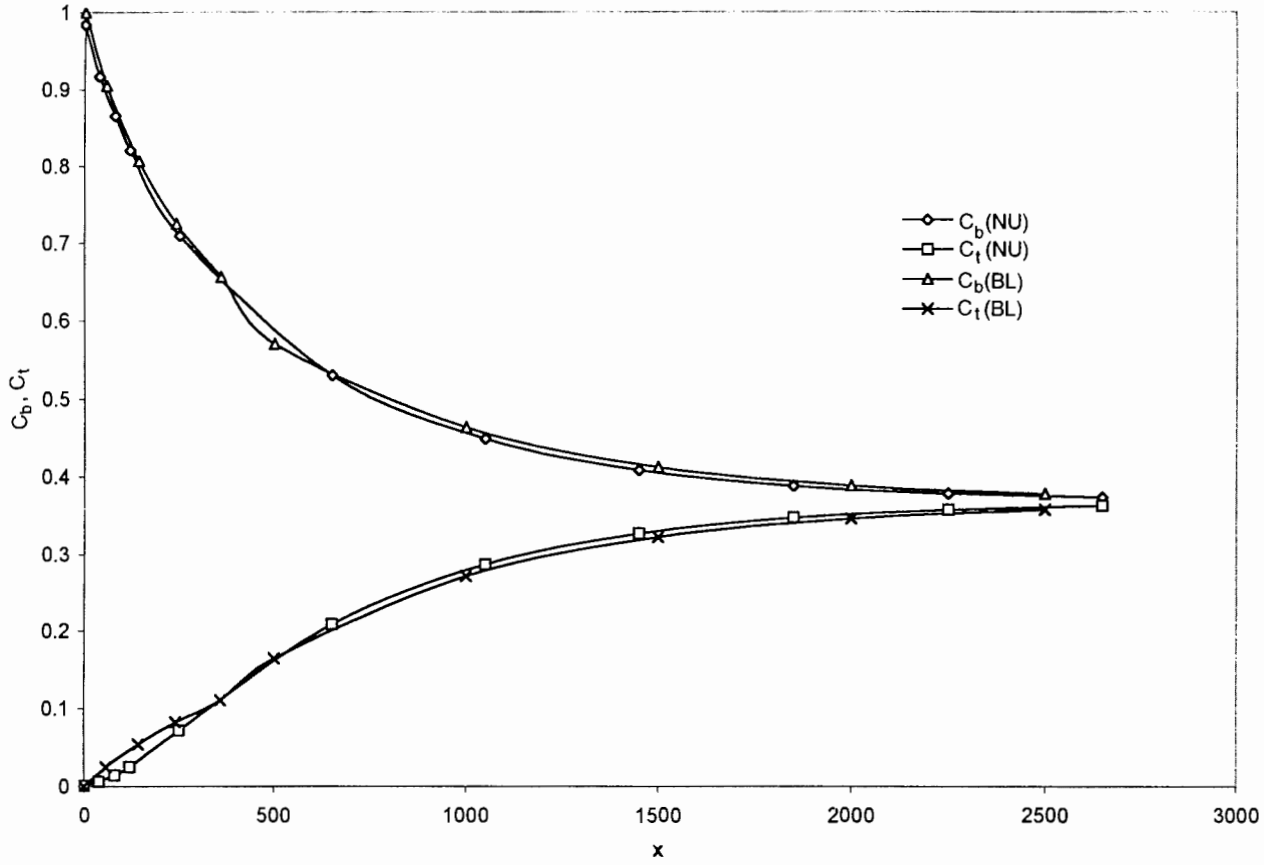

Figure 11d Comparison between the TSBL predictions (BL) referring to the restructuring and establishment sections and numerical results (NU).

(d) Variation of bottom and top salinity along the aquifer
Seepage of saltwater into the freshwater zone
(a=0.1; q_R =0.1; X_e, X_{ent} = 100 ; B=24; $0 \leq x \leq X_p$)

Discussion

The application of the TSBL method developed in the present paper is appropriate for initial evaluation of salinity transport in an aquifer subject to mineralization. The method can be helpful for quick evaluation of field data gathered by monitoring systems, and can be applicable to the design and implementation of monitoring systems for field data collection. Use of the boundary layer approach developed in this study permits the development of designs based on sparse or preliminary data.

The TSBL method can also be useful in determining which numerical model should be used for the simulation of salinity transport in an aquifer, since it potentially provides accurate predictions of the point of uniformity, where the salinity is uniformly distributed in the aquifer cross section. Downstream of that point salinity dispersion is dominated by longitudinal dispersion, and a basically two-dimensional modeling approach can provide adequate information about salinity transport. For example, in the specific case of salinity migration into the Equus Beds aquifer in south central Kansas, which led to the present research, the method developed in this study can help identify the appropriate region to incorporate into numerical modeling simulations.

Generally, it seems that field data collection aiming at the identification of physical parameters like the characteristic dispersivity are best carried out in regions located as close as possible to the source of saltwater, and/or in places characterized by comparatively large vertical salinity gradients. If data are collected in regions of significant salinity at the top of the aquifer, then vertical salinity gradients are probably small and longitudinal dispersion effects may be significant. Under such conditions evaluation of the aquifer characteristics cannot be accurate. In the restructuring section variations in the inner BL thickness are not simply related to dispersivity. In the establishment section, however, changes in salinity profiles are very moderate. Therefore, estimation of dispersivity values from field data is not recommended in either of these sections.

Summary and conclusions

This study concerns the horizontal penetration of salinity into an inland aquifer, where mineralization of the aquifer originates from the intrusion of salinity from deep formations into the freshwater zone. Downstream of the salinity intrusion location its plume is subject to advection with the aquifer flow, and to spreading in the vertical direction. It has been shown in previous studies that the top specified boundary layer (TSBL) can be very useful in the initial quantitative evaluation of the mineralization process as long as the mineralized zone is smaller than the aquifer thickness. In the present study, we consider the phenomena occurring downstream of the entrance cross section at the attachment point, where the top of the mineralized zone arrives at the top of the aquifer. Preliminary numerical experiments applied to appropriately defined, normalized salinity and vertical coordinates show that it is possible to identify two BLs (termed 'inner' and 'outer') in the aquifer cross section. Downstream of the entrance cross section, the inner BL expands, and the outer BL shrinks, until each one of them occupies half of the aquifer cross section, at the establishment point. We applied the TSBL method to obtain simplified expressions for the inner BL thickness, and for salinity values at the bottom and top of the aquifer. The basic formulations are based on the assumption that the evaluated domain could be divided into two sections: (a) a restructuring section, and (b) an establishment section. In the restructuring section there is no salinity transfer between the inner and outer BLs. In this section vertical salinity gradients lead to expansion of the inner BL, until it occupies half of the aquifer cross section. In the establishment section vertical salinity gradients only lead to salinity transfer from the inner to the outer BL, until the salinity is distributed uniformly in the aquifer cross section. It is shown that lengths of the restructuring and establishment sections are approximately proportional to the aquifer thickness squared, and are inversely proportional to the transverse dispersivity.

Comparisons between numerical simulations based on the solution of the equation of salinity transport in the aquifer and results obtained by the TSBL method have indicated the validity of the latter.

The study provides a convenient set of definitions and terminology that are helpful in visualizing the gradual development of uniform salinity distribution in an aquifer subject to mineralization.

The method developed in this study can be useful for the initial quantitative evaluation of a variety of issues associated with the penetration and spreading of contaminants in groundwater aquifers. It is anticipated that this method will be applicable in the initial evaluation of field data, design of field data collection and determination of adequate numerical modeling procedures for the analysis of transport phenomena in aquifers.

ACKNOWLEDGMENTS

This work was supported under contracts between the Kansas Water Office and the Kansas Geological Survey. The authors are grateful for the assistance of Mark Schoneweis in preparing the illustrations.

Notation

a	dimensions transverse dispersivity
B	dimensionless thickness of the aquifer
B^*	thickness of the aquifer[L]
c	normalized salinity defined in eq. (14)
C	relative salt concentration (salinity)
C_b	relative salinity at the bottom of the aquifer
C_t	relative salinity at the top of the aquifer
C^*	salt concentration (salinity) [ML^{-3}]
C_f^*	salinity of freshwater [ML^{-3}]
C_s^*	salinity of saltwater [ML^{-3}]
$\tilde{\tilde{D}}$	dispersion tensor [L^2T^{-1}]
D_x	longitudinal dispersion coefficient [L^2T^{-1}]
D_y	transverse dispersion coefficient [L^2T^{-1}]
F	function defined in eq. (54)
g	gravitational acceleration [LT^{-2}]
k	permeability [L^2]
l_0	unit length [L]
n, n_1, n_2	power coefficients
p	pressure [$ML^{-1}T^{-2}$]
q	specific discharge [LT^{-1}]
q_R	ratio between the specific discharges of the seeping saltwater and the aquifer

ROI region of interest - the top specified boundary layer

t dimensionless time

t^* time [T]

TSBL top specified boundary layer

V interstitial flow velocity [LT^{-1}]

x dimensionless longitudinal coordinate

X_e dimensionless length of the impermeable layer discontinuity

X_{ent} dimensionless distance between the upstream side of the impermeable layer discontinuity and the attachment point, which comprises the entrance cross section

X_p distance along which the uniform salinity profile is obtained

X_r dimensionless length of the restructuring section

x^* longitudinal coordinate [L]

X_e^* length of the impermeable layer discontinuity [L]

X_{ente}^* distance between the upstream side of the impermeable layer discontinuity and the entrance cross section [L]

y dimensionless vertical coordinate

y^* vertical coordinate [L]

α coefficient defined in eq. (47)

β_i (i=1,...5) coefficients defined in eq. (40)

γ coefficient defined in eq. (36)

δ dimensionless thickness of the ROI

δ_u dimensionless thickness of the inner boundary layer

ζ modified dimensionless vertical coordinate

η dimensionless coordinate of the outer boundary layer

μ fluid viscosity [$ML^{-1}T^{-1}$]

ρ fluid density [ML^{-3}]

ξ dimensionless coordinate of the inner boundary layers

References

Buddemeier, R.W., Garneau, G.W., Healey, J.M., Ma T.-S., Sophocleous, M.A., Wittemore, D.O., Young, D.P., and Zehr, D., 1993. The mineral intrusion project - report of progress during fiscal year 1993, Open-file Report 93-23, Kansas Geological Survey, The University of Kansas, Lawrence, Kansas.

Buddemeier, R.W., Falk, S., Garneau, G.W., Laterman, J., Ma, T.-S., Sophocleous, M.A., Whittemore, D.O., Young, D.P., and Zehr, D., 1994. The mineral intrusion project: investigation of salt contamination of ground water in the eastern Great Bend Prairie aquifer - progress and activities during fiscal year 1994, Open-file Report 94-28, Kansas Geological Survey, The University of Kansas, Lawrence, Kansas.

Carslaw, H.S., and Jaeger, J.C., 1959. "Conduction of Heat in Solids," Oxford at the Clarendon Press, London.

Fischer, H.B., List, E., Koh, R.C.Y., Imberger, J. and Brooks, N.H., 1979. Mixing in Inland and Coastal Waters, Academic Press, NY.

Garneau, G.W., 1995. Detection and characterization of the distribution of mineral intrusion in the Great Bend Prairie aquifer - south-central Kansas, Open-file Report 95-35, Kansas Geological Survey, The University of Kansas, Lawrence, Kansas.

Hill, J.M., and Dewynne, J.N., 1987. "Heat Conduction," Blackwell Scientific, Oxford, U.K.

Rubin, H., and Buddemeier, R.W., 1996. A top specified boundary layer (TSBL) approximation approach for the simulation of groundwater contamination processes, accepted for publication in J. of Contaminant Hydrology, 22: 123 – 144.

Rubin, H., and Buddemeier, R.W., 1998a. Application of the top specified boundary layer (TSBL) approximation to initial characterization of an inland aquifer mineralization- Part 1: Direct contact between fresh and saltwater, Journal of Contaminant Hydrology, 32/3-4: 149-172.

Rubin, H., and Buddemeier, R.W., 1998b. Application of the top specified boundary layer (TSBL) approximation to initial characterization of an inland aquifer mineralization-Part 2: Seepage of saltwater through semi-confining layers, Journal of Contaminant Hydrology, 32/3-4: 173-198.

Rubin, H., and Buddemeier, R.W., 1998c. Approximate analysis of groundwater mineralization due to local discontinuities in impermeable layer - Part 1 Direct contact between fresh and saltwater, Open-file Report 98-31, Kansas Geological Survey, The University of Kansas, Lawrence, Kansas.

Rubin, H., and Buddemeier, R.W., 1998d. Approximate analysis of groundwater mineralization due to local discontinuities in impermeable layer - Part 2: Seepage of saltwater through semi-confining discontinuity, Open-file Report 98-32, Kansas Geological Survey, The University of Kansas, Lawrence, Kansas.

USBR (U.S. Bureau of Reclamation), 1993. Arkansas River water management improvement Study - modeling of chloride transport in the Equus Beds aquifer, Technical Report, Denver, Colorado

Whittemore, D.O., and Sophocleous, 1995. Hydrologic and chemical interaction of the Arkansas River and the Equus Beds aquifer between Hutchinson and Nickerson - north-central Reno County Kansas, Appraisal investigation, Kansas Geological Survey, The University of Kansas, Lawrence, Kansas.